From Visibilities to Images
Tom Muxlow, JBCA

Practical guide to basic imaging
– Complimenting ‘Fundamental Interferometry’ & ‘Data Acquisition & Calibration’ talks

Initial Calibration:
- RFI excision, delay calibration, band-pass correction, gain & phase calibration, self-calibration

Imaging:
- image de-convolution, gridding schemes, wide-fields, non-coplanar baselines and multi-faceted images, chromatic aberration, mosiacing

High Fidelity Imaging:
- confusion, multi-frequency synthesis, high dynamic range imaging

Example data used from new wide-bandwidth arrays (ALMA, EVLA, LOFAR, *e*-Merlin….)

Initial Calibration: RFI Excision

– New broad-band interferometers operate well outside protected radio astronomy bands!!

Lower frequency observing bands tend to suffer more RFI problems

Many software packages have interactive RFI excision – but time consuming!!

Automatic scripting is being developed – after initial template flagging - *known RFI*

e-Merlin L-Band (8x64MHz IFs):

512MHz (1254 – 1766 MHz) BW

512 x 125kHz channels per IF

Transient & persistent RFI seen

Persistent RFI can be flagged for Target from calibration-scans

Bad RFI channels usually follow antennas – but magnitude is baseline and polarization dependent

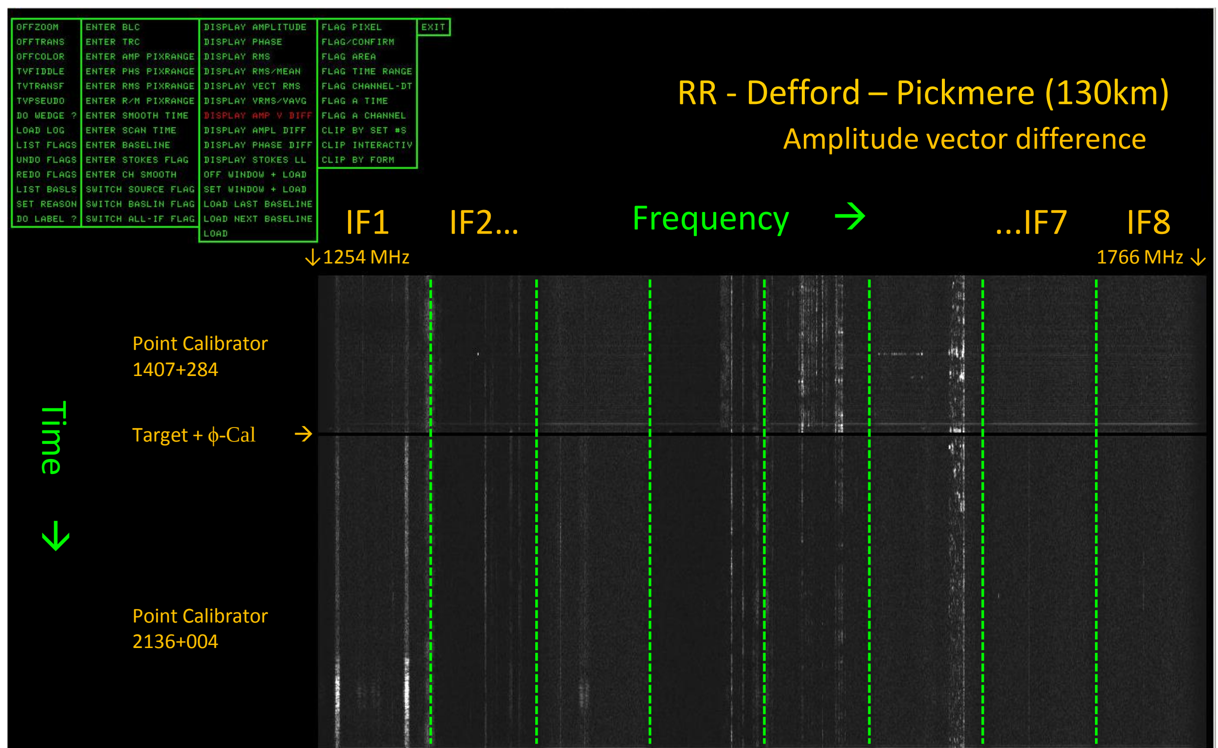

Initial Calibration: RFI Excision

– New broad-band interferometers operate well outside protected radio astronomy bands!!

Lower frequency observing bands tend to suffer more RFI problems

Many software packages have interactive RFI excision – but time consuming!!

Automatic scripting is being developed – after initial template flagging - *known RFI*

e-Merlin L-Band (8x64MHz IFs):

512MHz (1254 – 1766 MHz) BW

512 x 125kHz channels per IF

Large RX headroom ensures linearity (+ 8-bit digitisation)

Typically only lose 10-15% of total passband

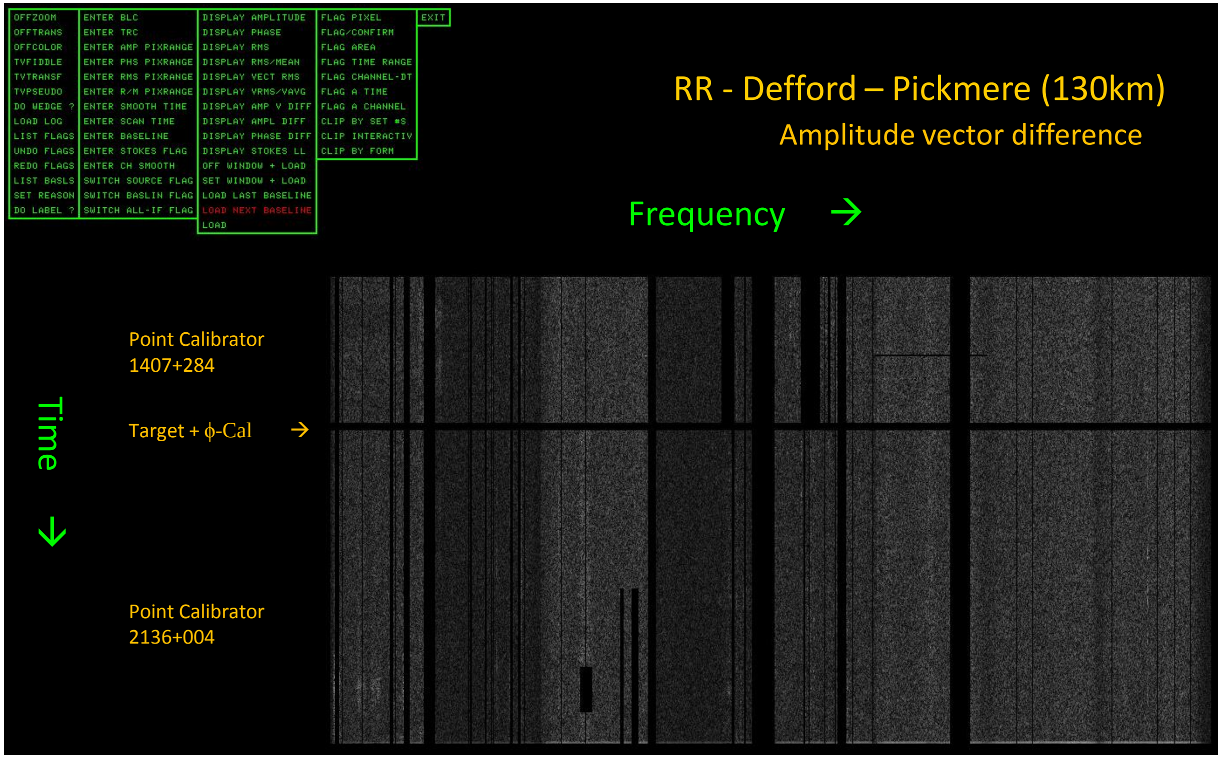

Initial Calibration: Delay Correction

Not geometric (Earth rotation) delay applied in correlator
– data transport / electronic delays from distant antennas

Wide-band data from many telescopes delivered with delay correction applied

Some instruments (EVN, *e*-Merlin….) require delay corrections to be calculated at an early stage of data reduction – using sources with good s:n (usually calibrators)

Lo – Kn (RR) Lo – Kn (LL) IFs →

ϕ

A

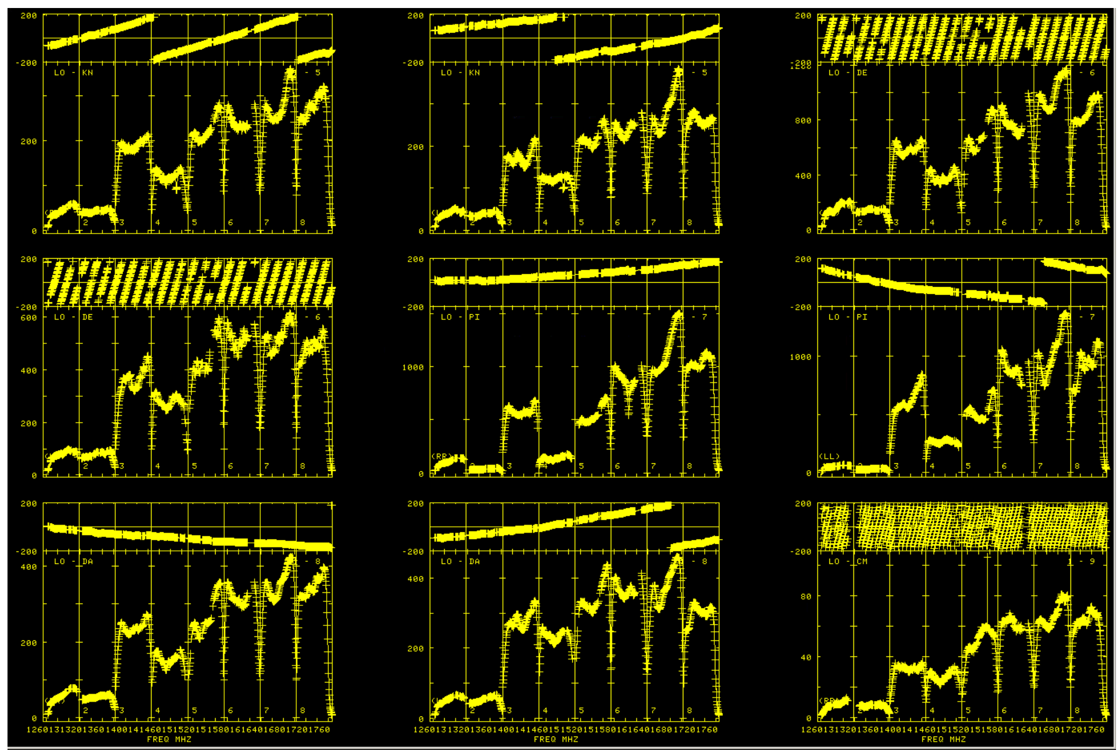

Multi-IF spectral plots of raw data will show delay errors from phase slopes across the pass-band

Single or multi-IF delays can be found (usually multi-IF unless you expect different delays for each IF)

Initial Calibration: Delay Correction

Wide-band data from many telescopes delivered with delay correction applied

Some instruments (EVN, *e*-Merlin….) require delay corrections to be calculated at an early stage of data reduction – using sources with good s:n (usually calibrators)

Use unaveraged data for accurate large delay solutions
→ data are Nyquist sampled

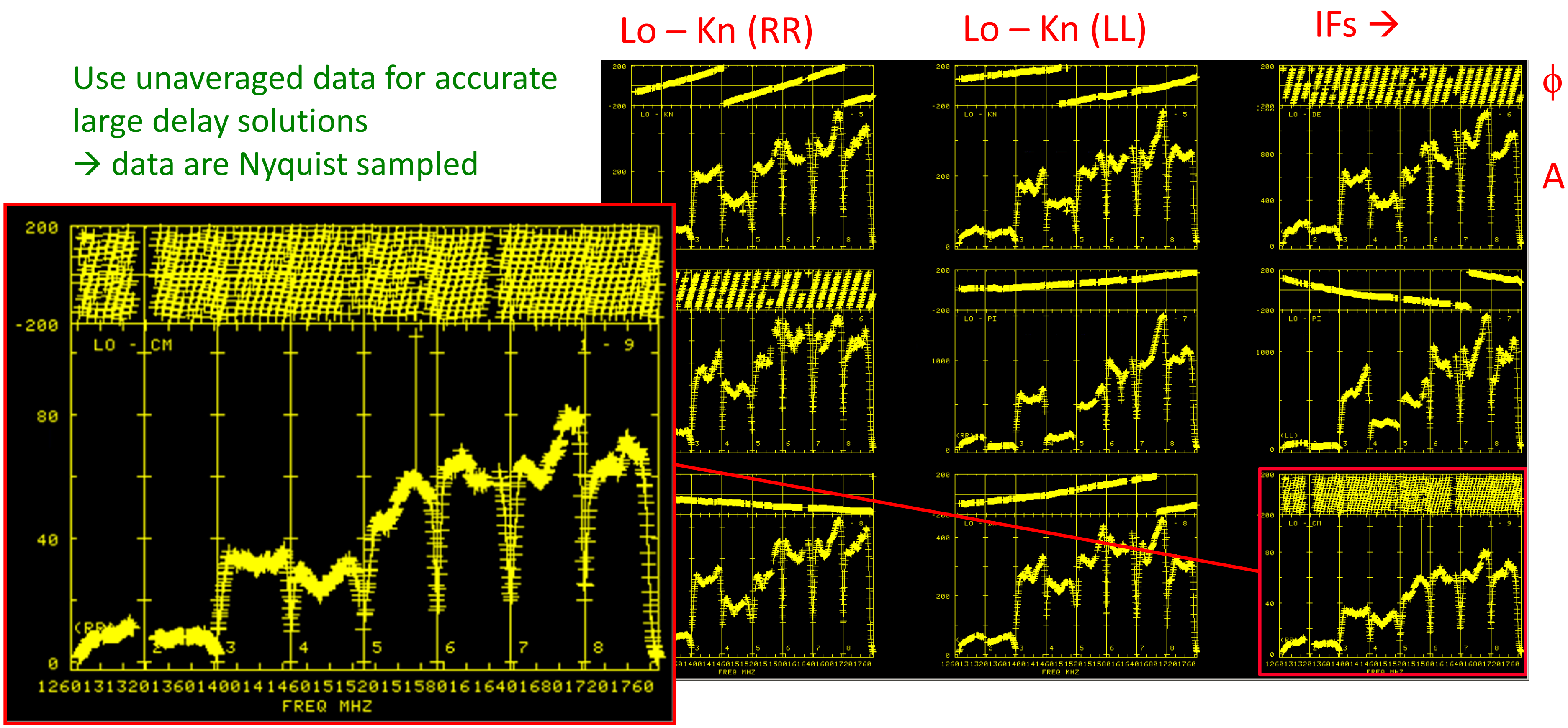

Initial Calibration: Gain Calibration

Point source primary calibrators – variable (t ~days - months)
Flux density calibrator – not variable but resolved (modelled)
Phase calibrator (secondary) – observed often (near point-like)

Amplitude scale usually set by primary and flux density calibrators
Delays from any calibrator with reasonable s:n
Phases (& gain tweaks) for target from phase-cal (8:2 min cycle)

Final fine adjustments made through band-pass calibration (bright calibrators only) to flatten the IF responses

Corrected data on 1407+284 after final delay, phase, gain, and bandpass corrections

1407+284 has a rising spectrum

Some RFI still present - IFs 1&2

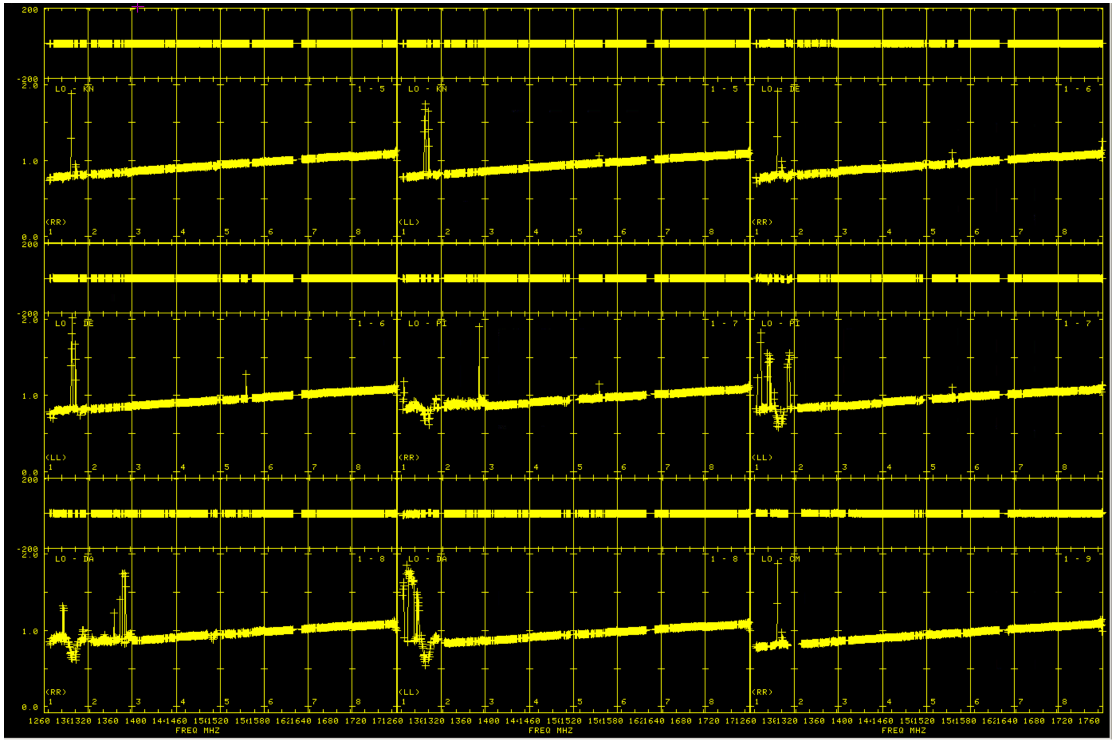

Point calibrator 1404+284

Initial Calibration: Gain Calibration

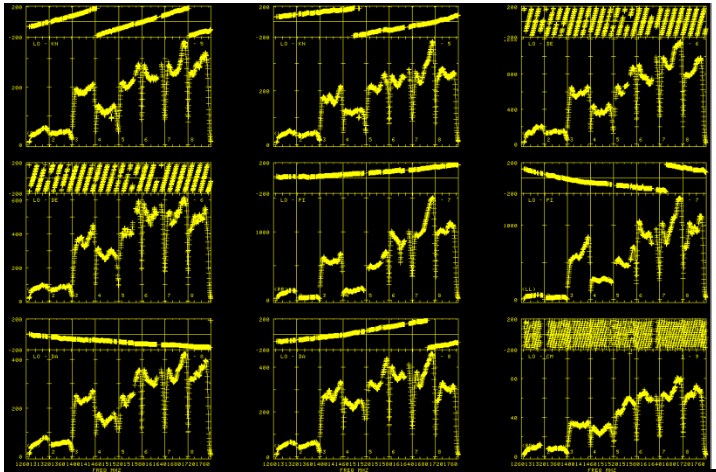

← Before

After ↓

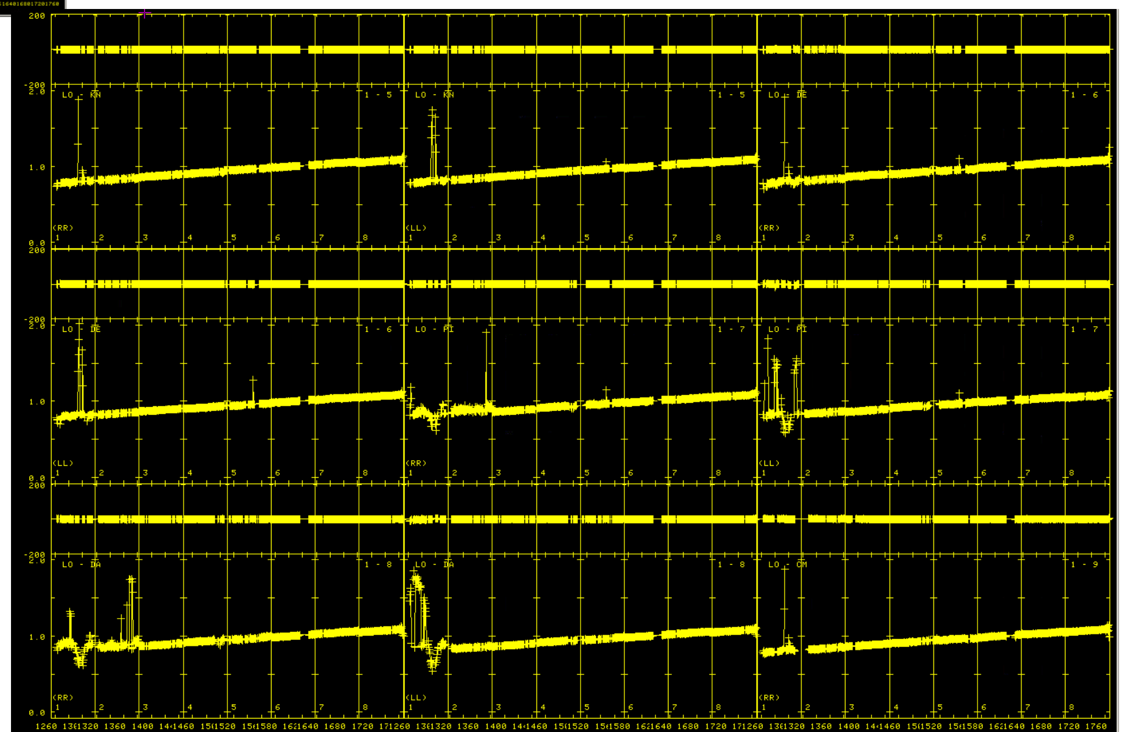

Point calibrator 1404+284

Final fine adjustments made through band-pass calibration (bright calibrators only) to flatten the IF responses

Passband-corrected data on 1407+284 after final delay, phase, gain, and bandpass corrections

1407+284 has a rising spectrum

Some RFI still present - IFs 1&2

Initial Calibration: Phase Calibration

Phase solutions (relative to reference antenna) from phase calibration source
→ phase calibration for the Target source → instrument phase stable and allows initial imaging

e-MERLIN image – DQSO observed at 6.5-7.0 GHz

- highest resolution image of kpc jet yet made

- imaged in CASA

- final image quality depends on refining the initial calibration sequence...

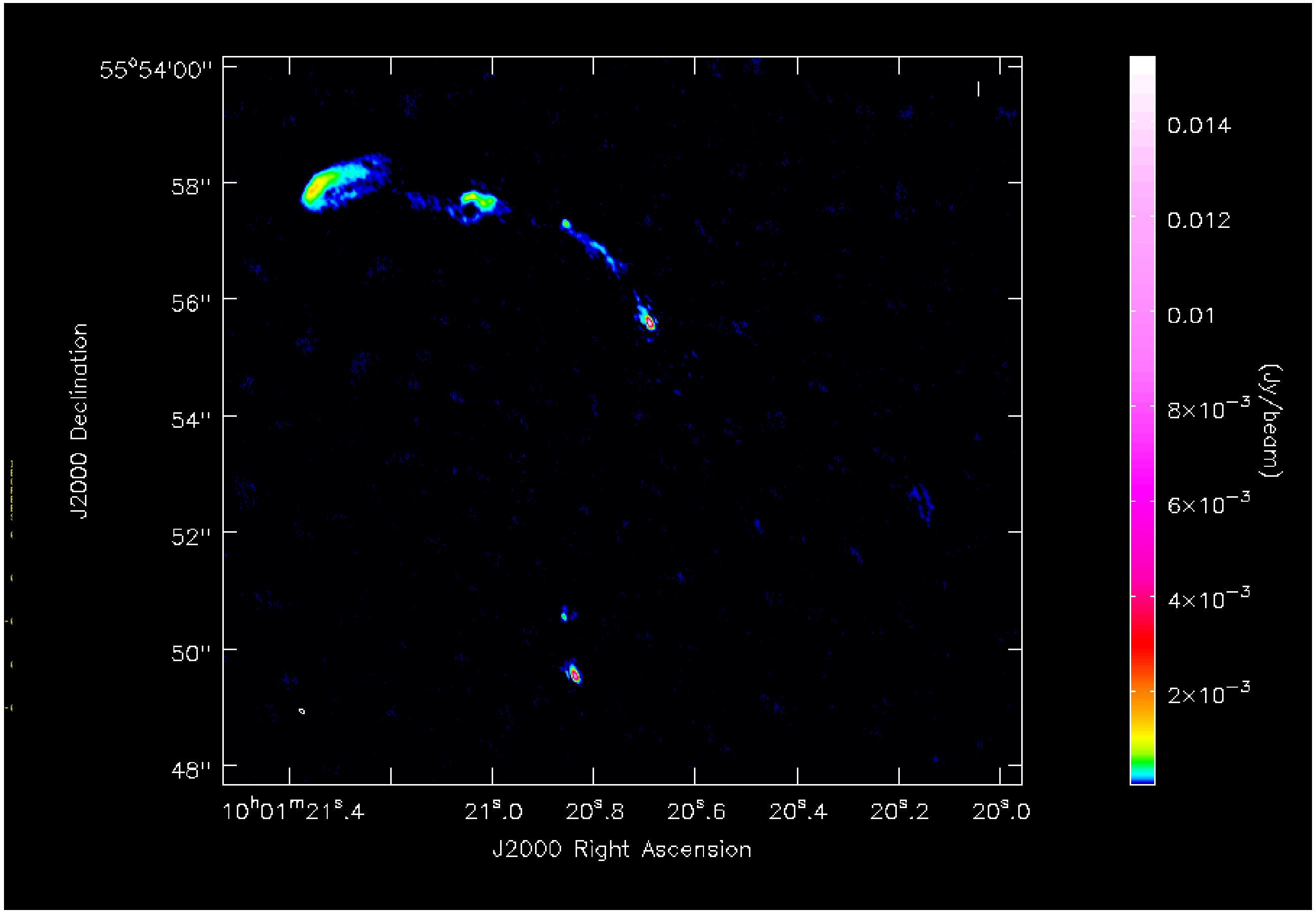

Initial Calibration: Self-Calibration – 1

Image target source after applying initial phase & gain solutions

If target is bright enough, use the initial target image to apply further self-calibration refinements to the phase and gain solutions

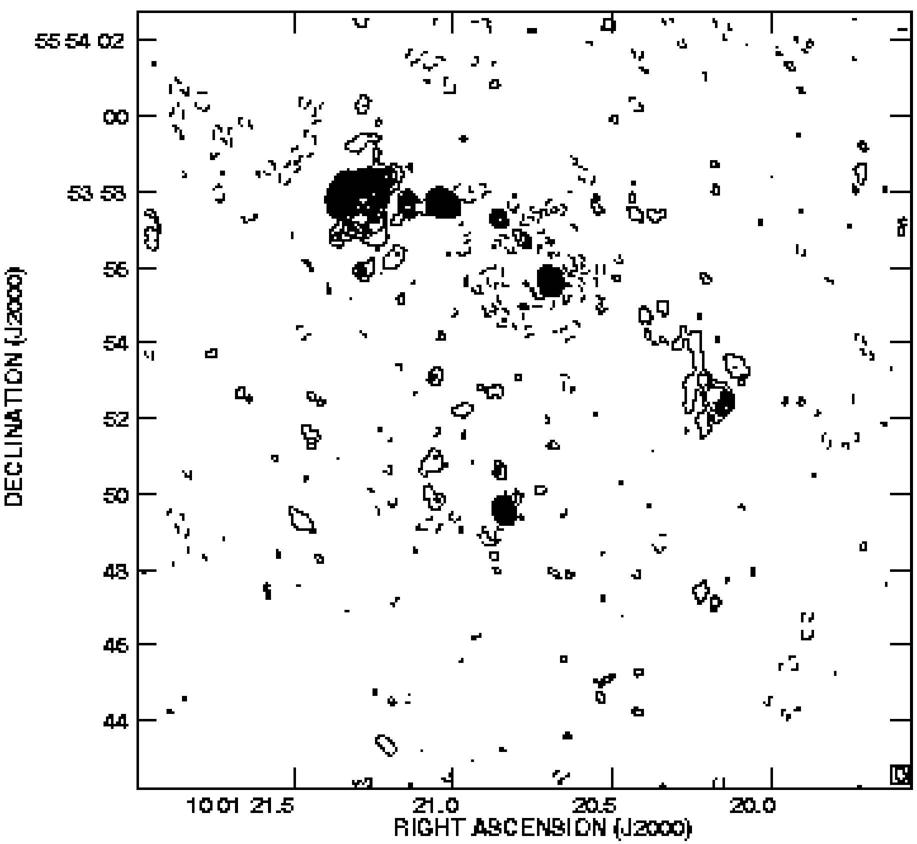

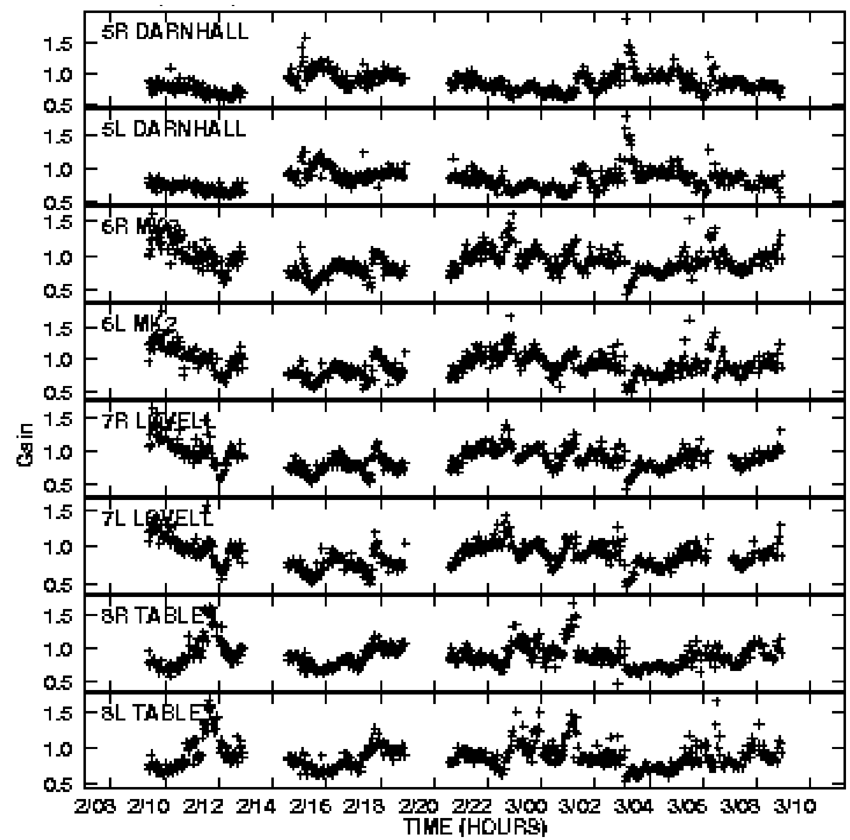

Initial Calibration: Self-Calibration – 2

During self-calibration, if troubled by side-lobes, use windowing to restrict positions of source model components.

Include components to first negative and restrict *u-v* range to match flux in model

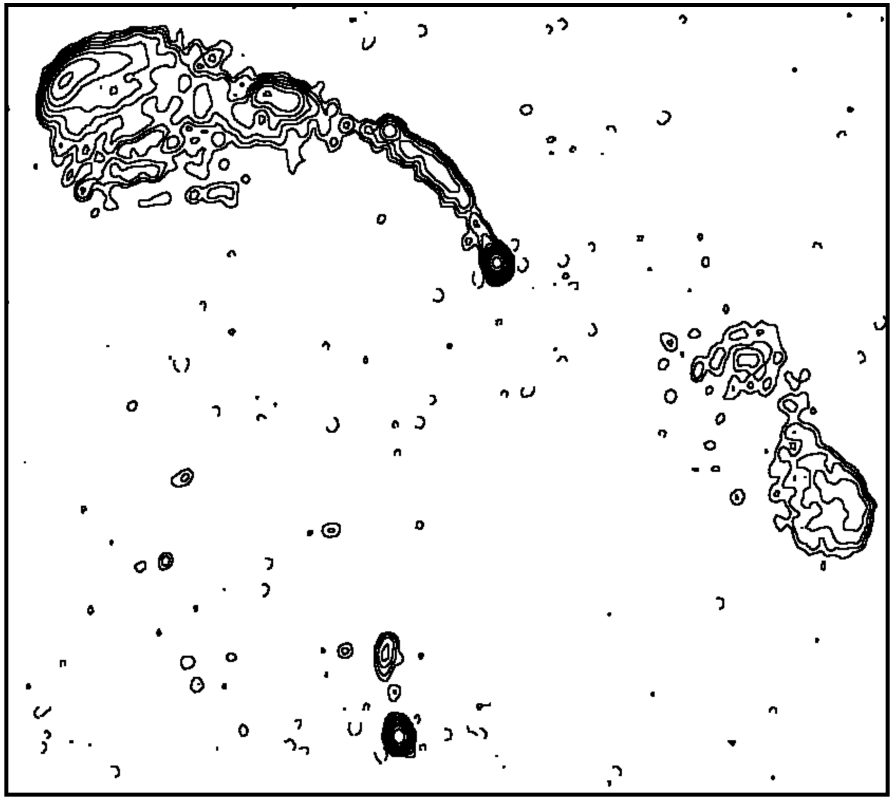

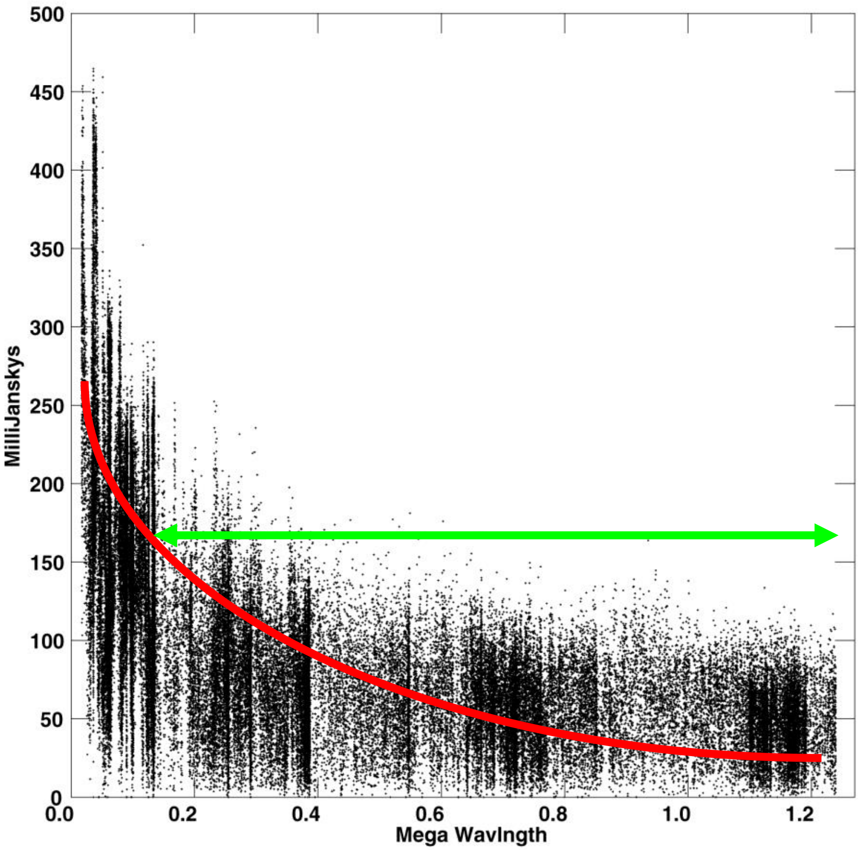

Initial Calibration: Self-Calibration – 2

During self-calibration, if troubled by side-lobes, use windowing to restrict positions of source model components.

Include components to first negative and restrict *u-v* range to match flux in model

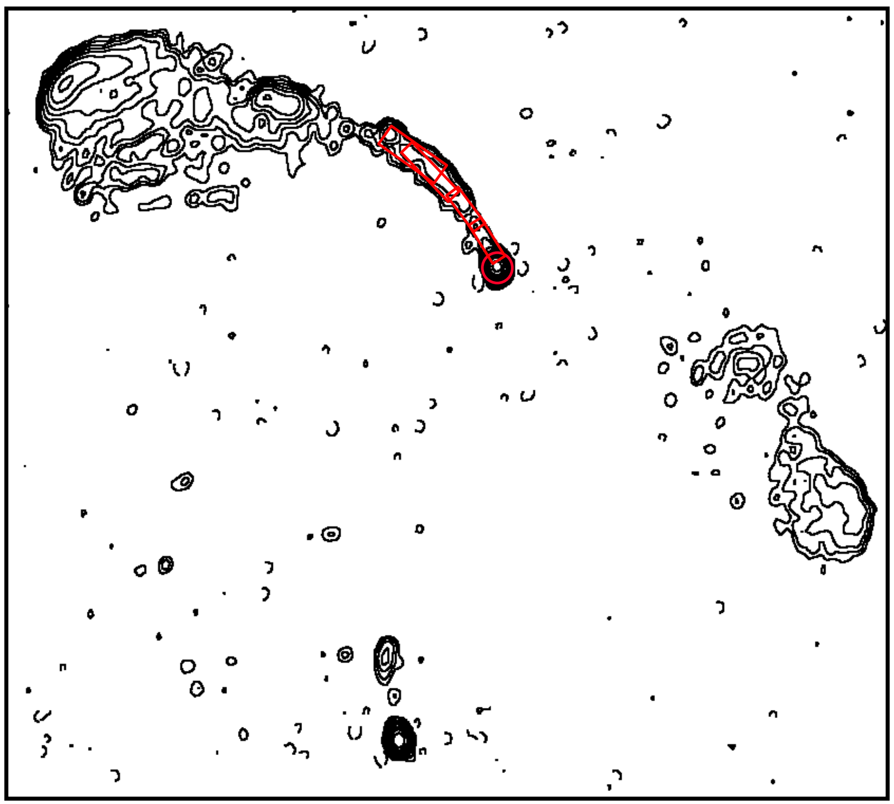

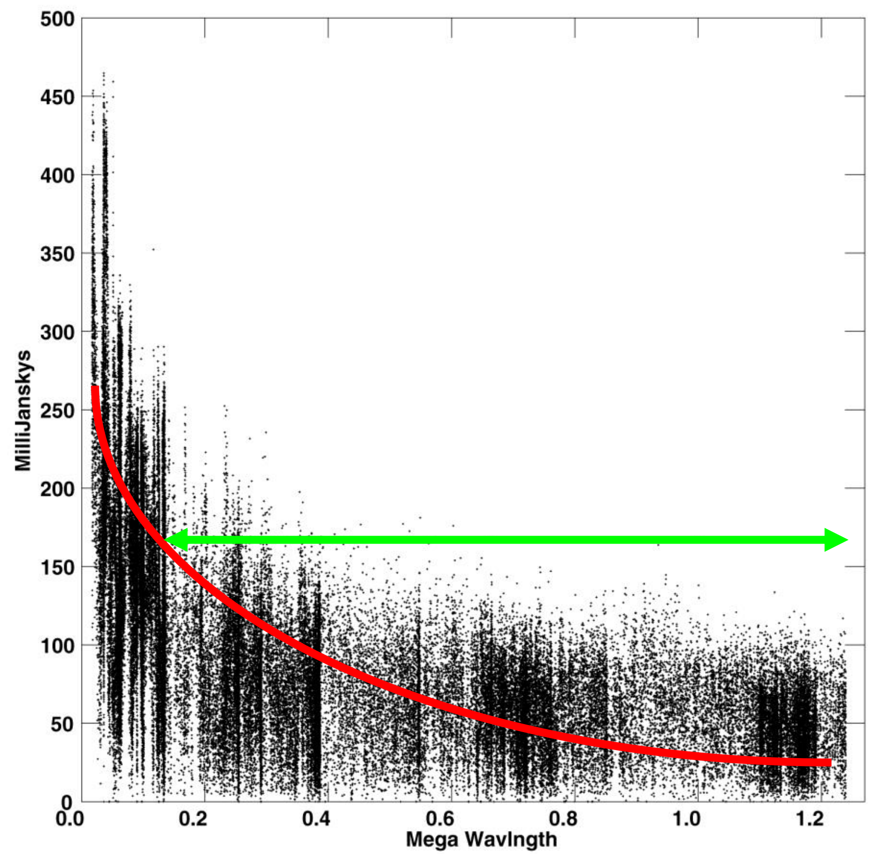

Imaging: Deconvolution

Unsampled regions in the telescope aperture give rise to severe ripples in the beam response (psf)

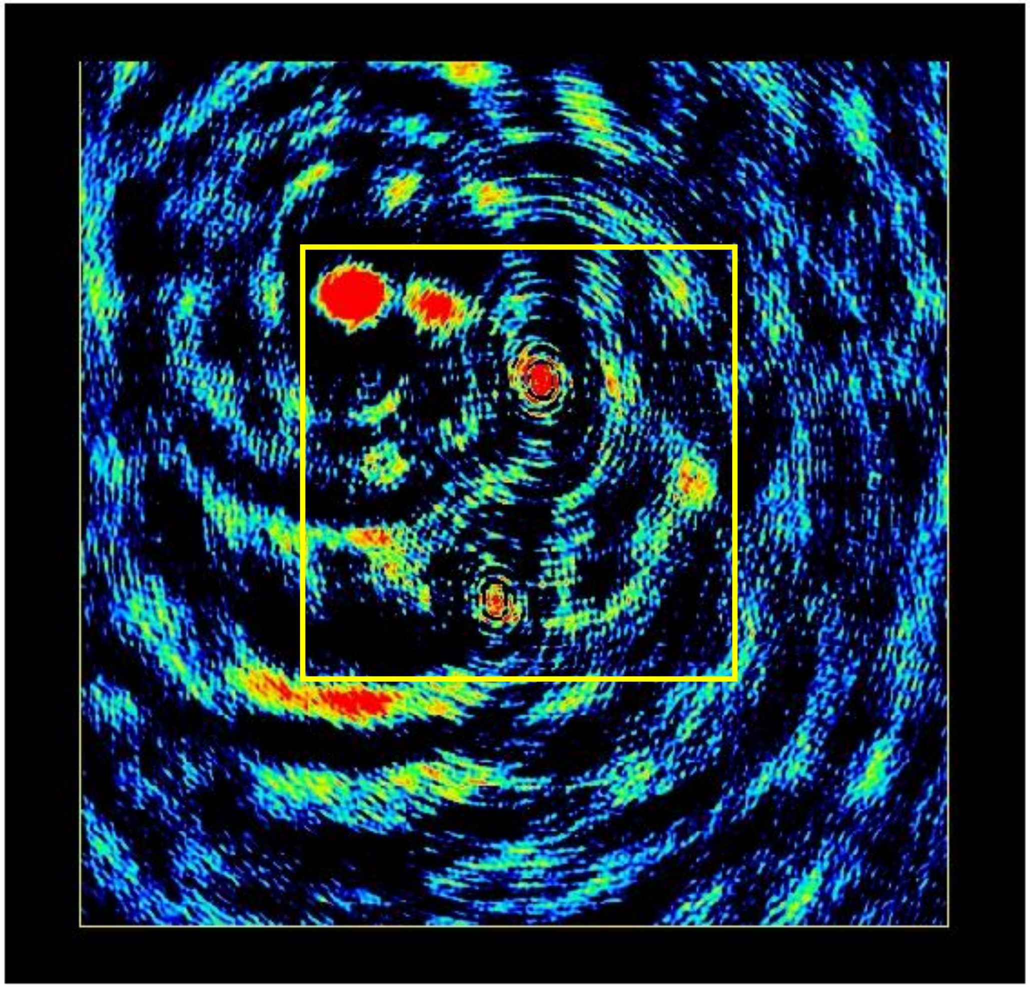

The raw Fourier-transformed image (dirty map) will usually require significant deconvolution

Conventional image-plane based algorithms will require a significant guard band around the source structure to avoid aliasing problems – typically restricted to the inner quarter

Visibility-based algorithms are able to tolerate such errors and typically allow imaging to within a few pixels of the edge of the image

Imaging: Deconvolution

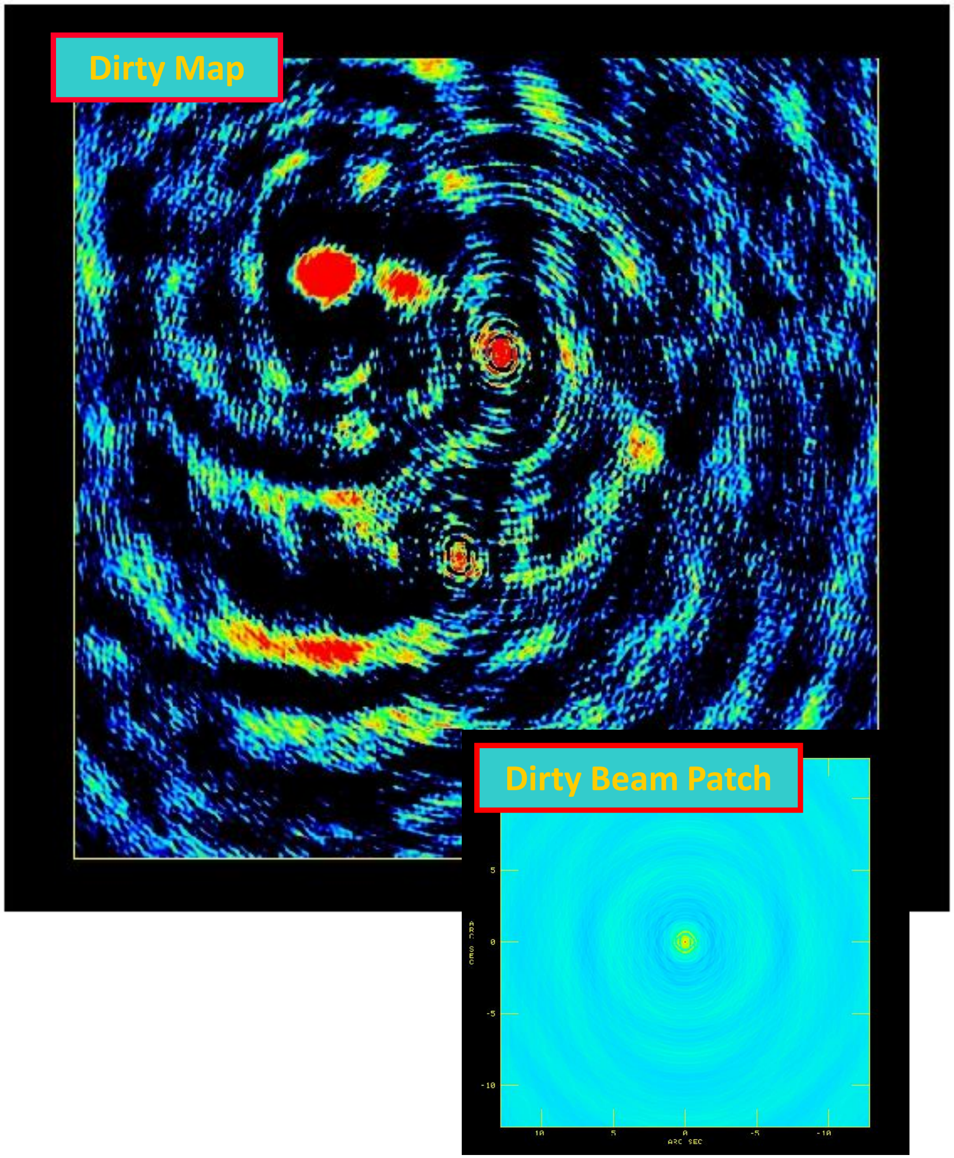

Conventional cleaning – centre the dirty beam under the peak of the dirty map and subtract the pattern scaled by 0.1 – continue until residual image is ~noise

Visibility-based algorithms subtract smaller beam patches which are then Fourier transformed back to the data plane and (vector) subtracted before re-gridding and transforming to form a new residual image

In both cases idealised point components smoothed by the fitted beam-shape are restored to the final residual image where each subtraction was performed

Imaging: Deconvolution – Extended Emission

RadioNet

Low surface brightness extended structure, can be subject to fragmentation during deconvolution
– especially for historical arrays with sparse *u-v* coverage

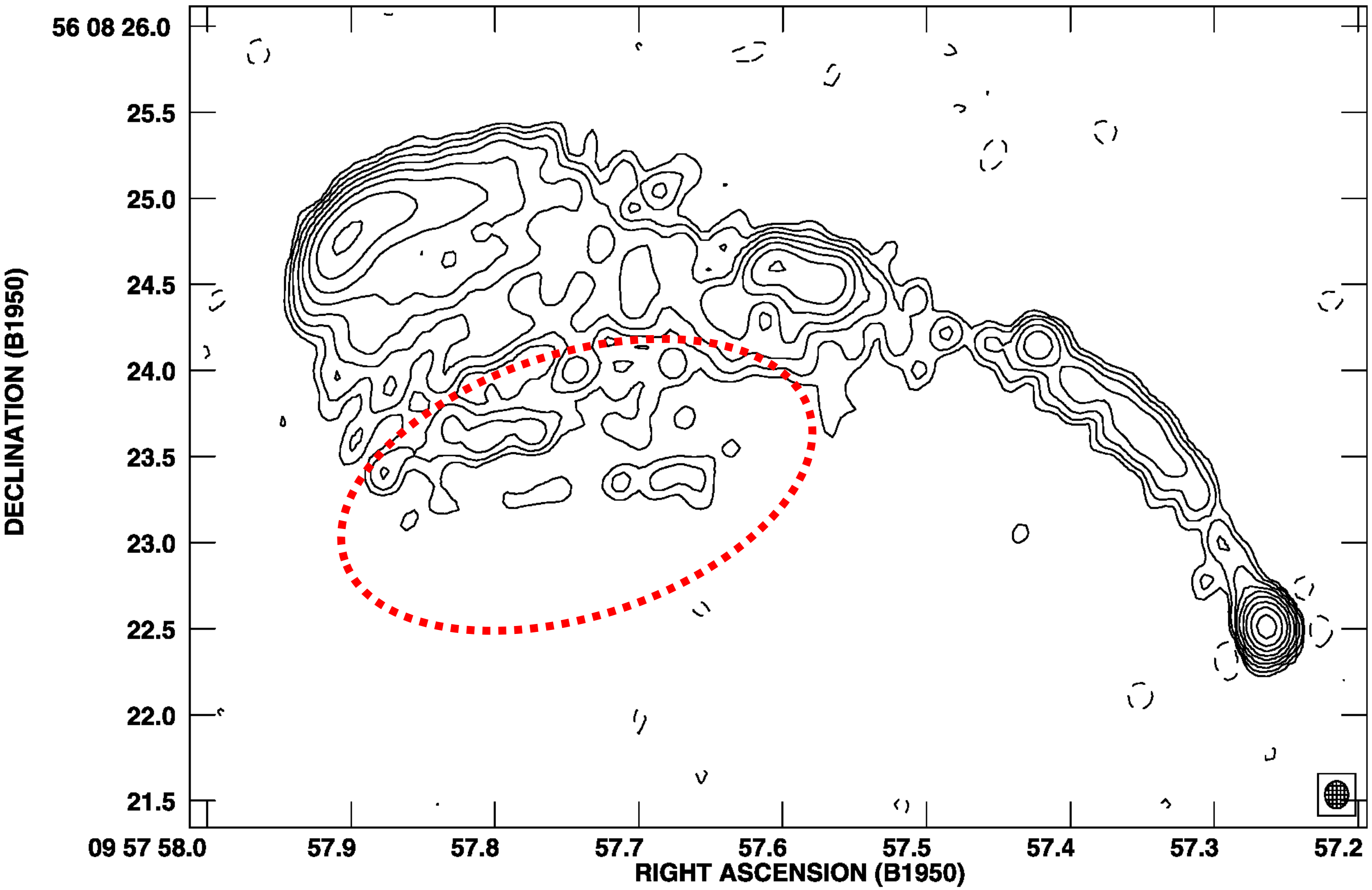

Imaging: Deconvolution – Extended Emission

Multi-scale CLEAN as implemented in AIPS and CASA produces superior results to conventional clean for complex extended structure

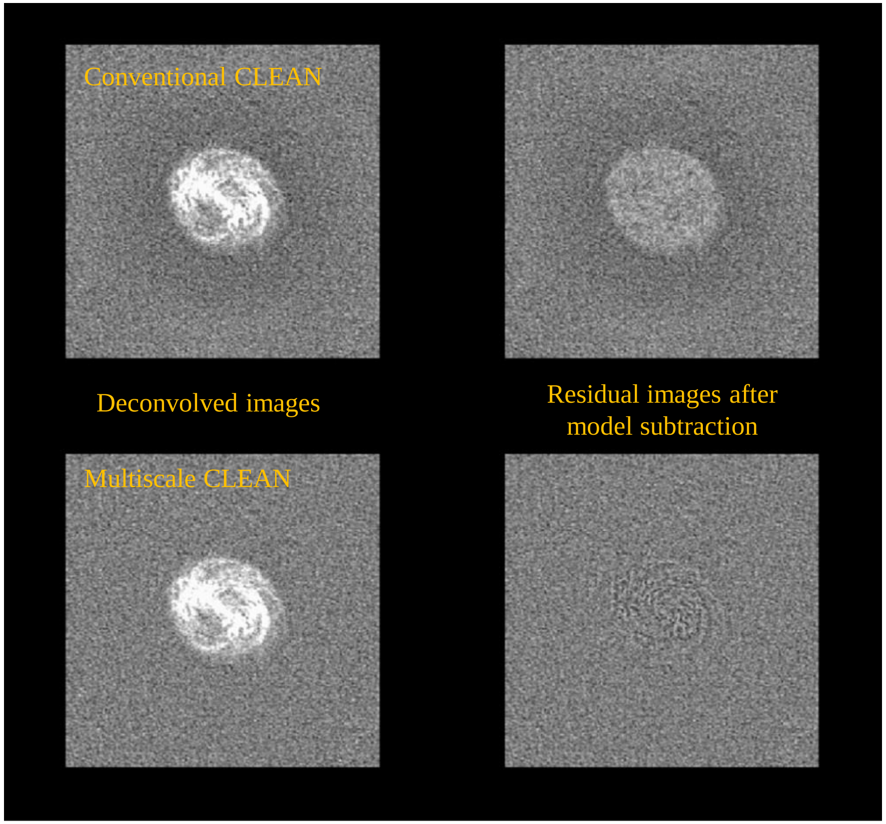

Residual image and beam smoothed to a selection of scale sizes (eg 0,2,4,8,16,32... pixels)

For each scale find strength & location of peak

For scale with maximum residual, subtract & add this component to source model

Update all residual images and loop around until peak residual flux reaches noise threshold (4σ)

Can produce very fine images from datasets containing large spatial frequency ranges – needs careful steering for sparsely filled aperture data...

Imaging: Deconvolution – Extended Emission

Multi-scale CLEAN as implemented in AIPS and CASA produces superior results to conventional clean for complex extended structure

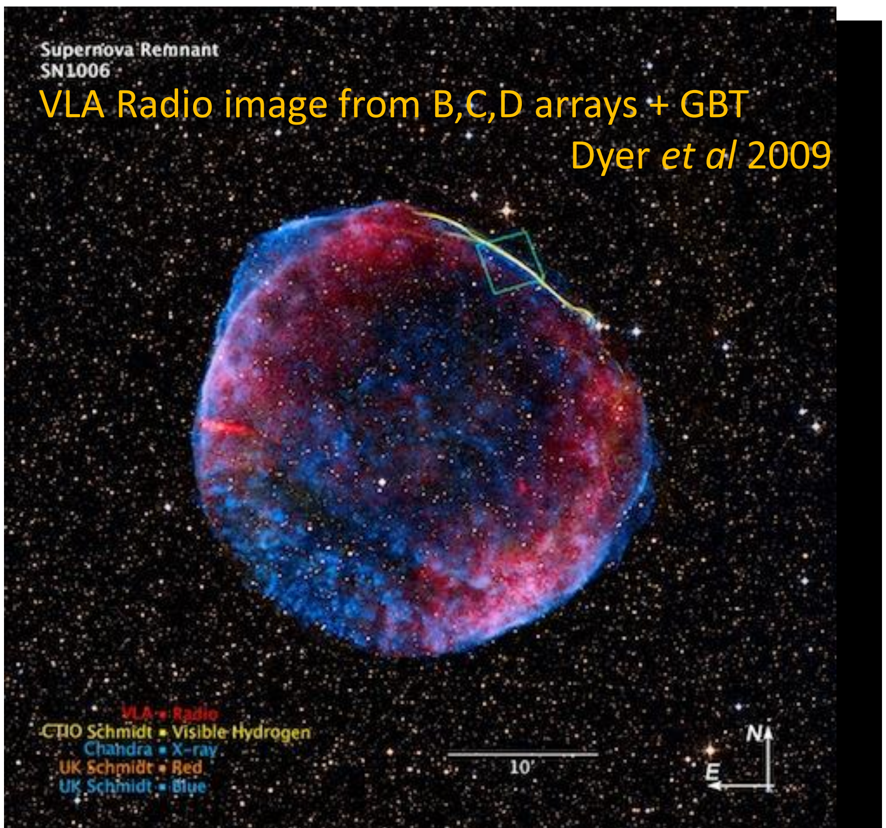

Residual image and beam smoothed to a selection of scale sizes (eg 0,2,4,8,16,32... pixels)

For each scale find strength & location of peak

For scale with maximum residual, subtract & add this component to source model

Update all residual images and loop around until peak residual flux reaches noise threshold (4σ)

Can produce very fine images from datasets containing large spatial frequency ranges – needs careful steering for sparsely filled aperture data...

Imaging: Deconvolution – Extended Emission

Multi-scale CLEAN as implemented in AIPS and CASA produces superior results to conventional clean for complex extended structure

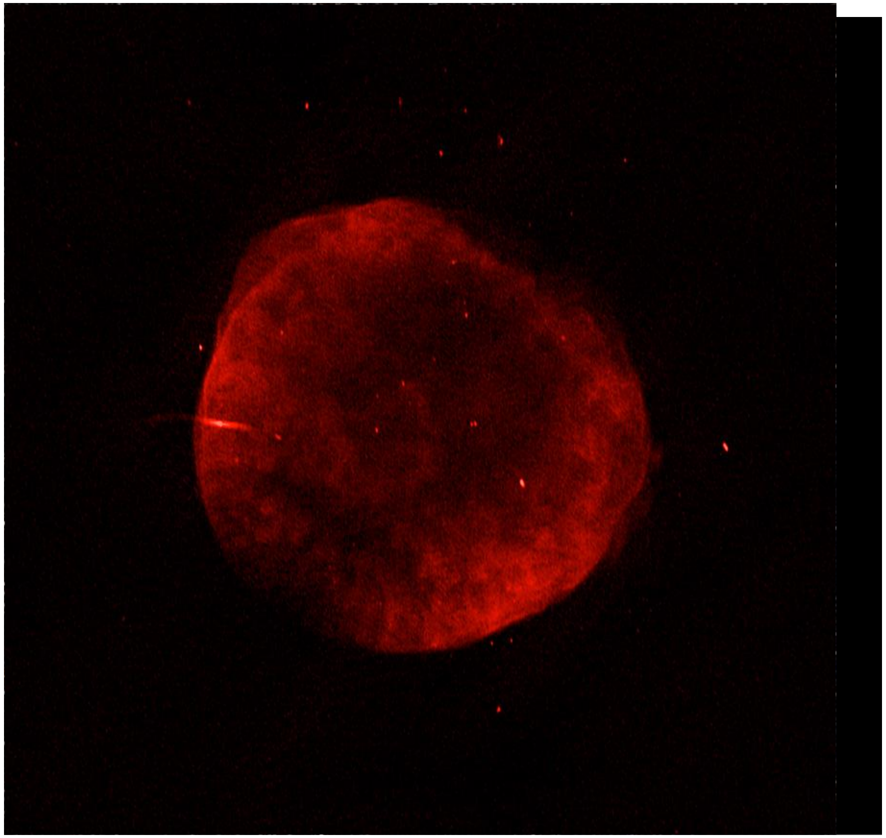

Residual image and beam smoothed to a selection of scale sizes (eg 0,2,4,8,16,32... pixels)

For each scale find strength & location of peak

For scale with maximum residual, subtract & add this component to source model

Update all residual images and loop around until peak residual flux reaches noise threshold (4σ)

Can produce very fine images from datasets containing large spatial frequency ranges – needs careful steering for sparsely filled aperture data...

Imaging: Data Gridding – 1

Integrations are distributed over a greater number of sampled grid points in the outer *u-v* plane than in the inner regions

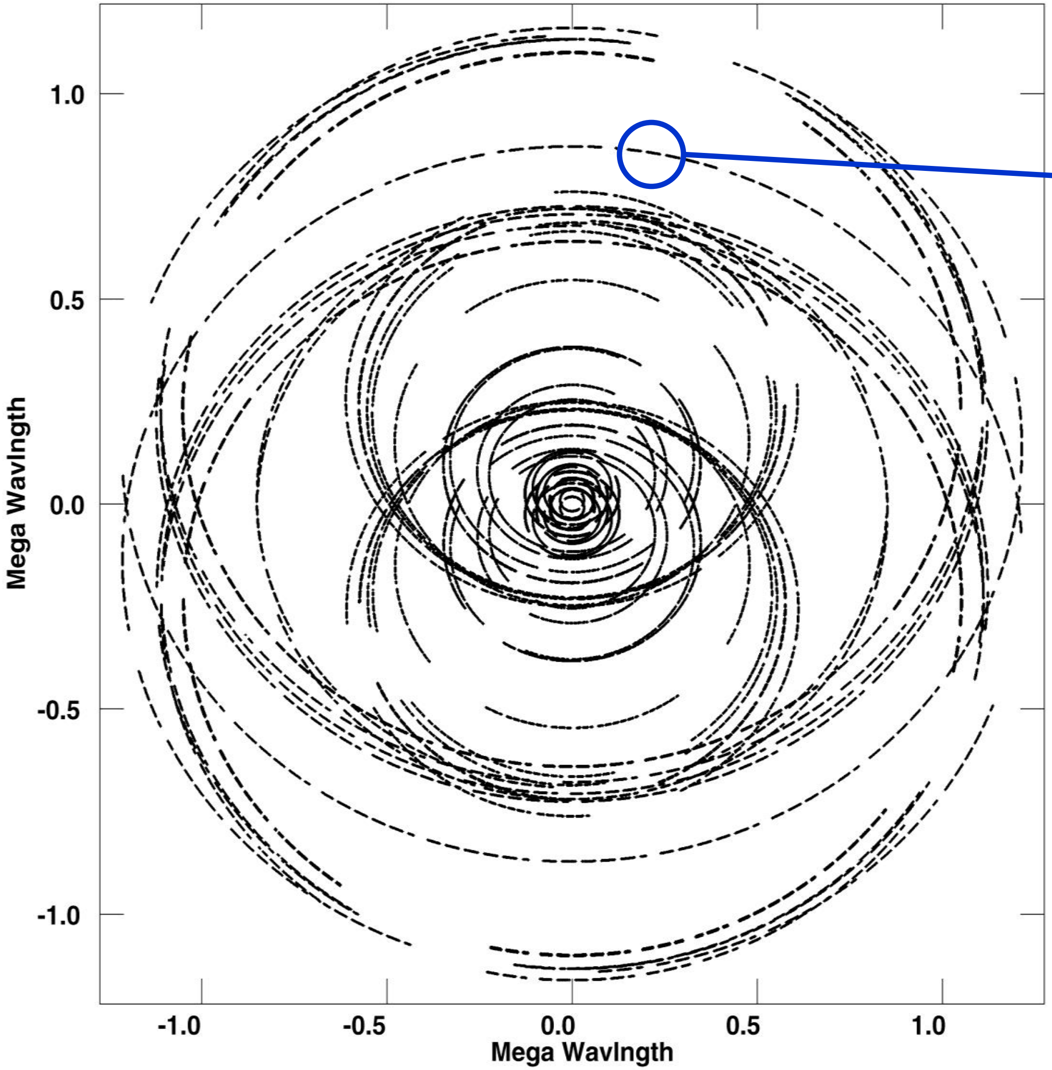

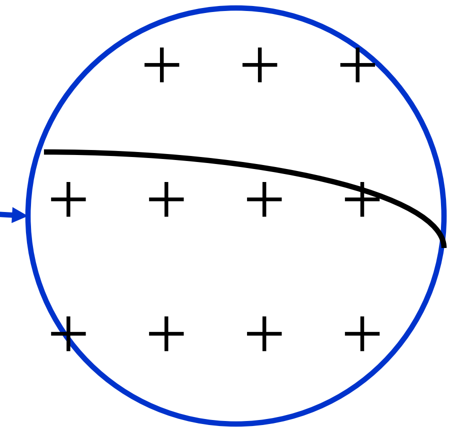

Data are interpolated onto a regular 2^n grid with a spheroidal convolution function

Weights unmodified by local density – 'Natural' weighting

Weights divided by local density of points – 'Uniform' weighting

Imaging: Data Gridding – 2

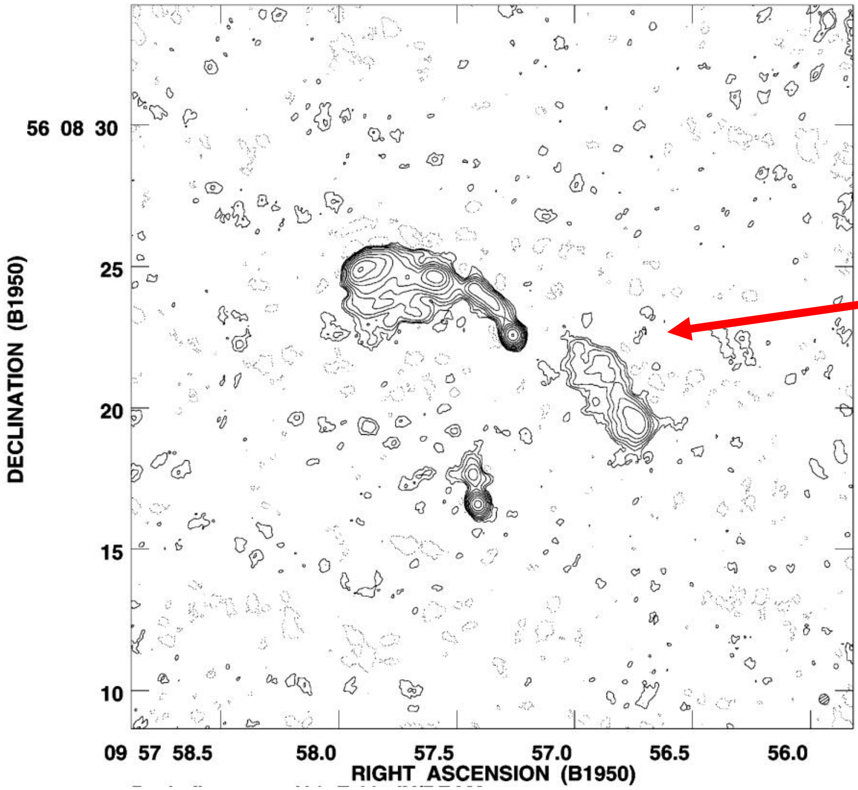

Naturally weighted images will give better sensitivity at the expense of angular resolution – low spatial frequencies are weighted up & data are utilised optimally

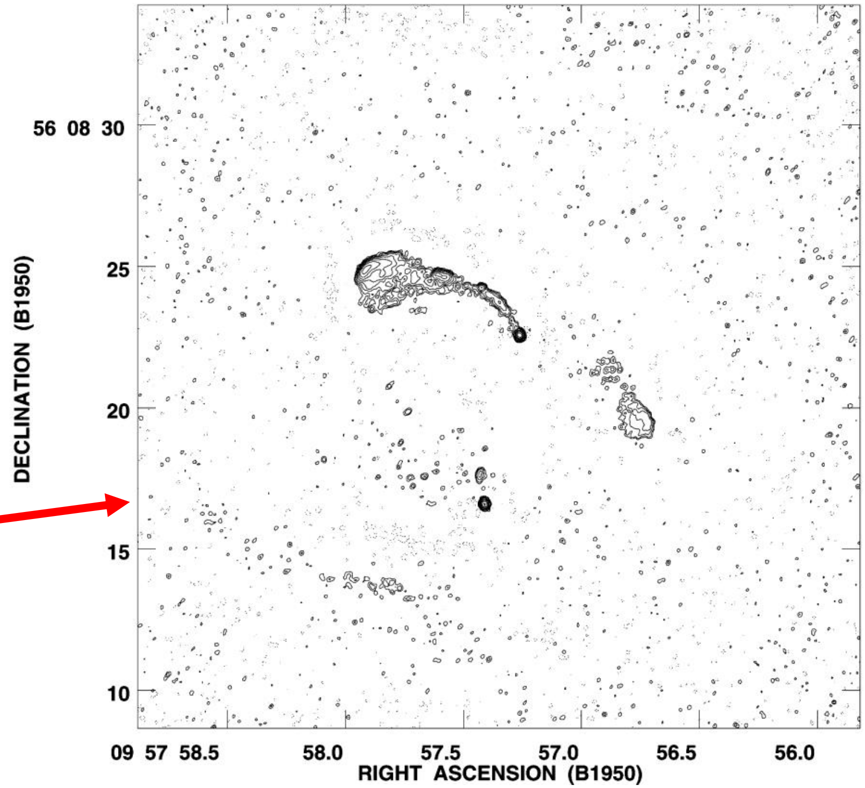

Uniformly weighted images will give better angular resolution at the expense of sensitivity – low spatial frequencies are weighted down and the data are not utilised optimally

– may be subject to a striping instability

Imaging: Data Gridding – Robustness

Originally derived as a cure for striping instability
– Natural weighting is immune and therefore most 'robust'

Robustness varies effective weighting as a function of local *u-v* weight density

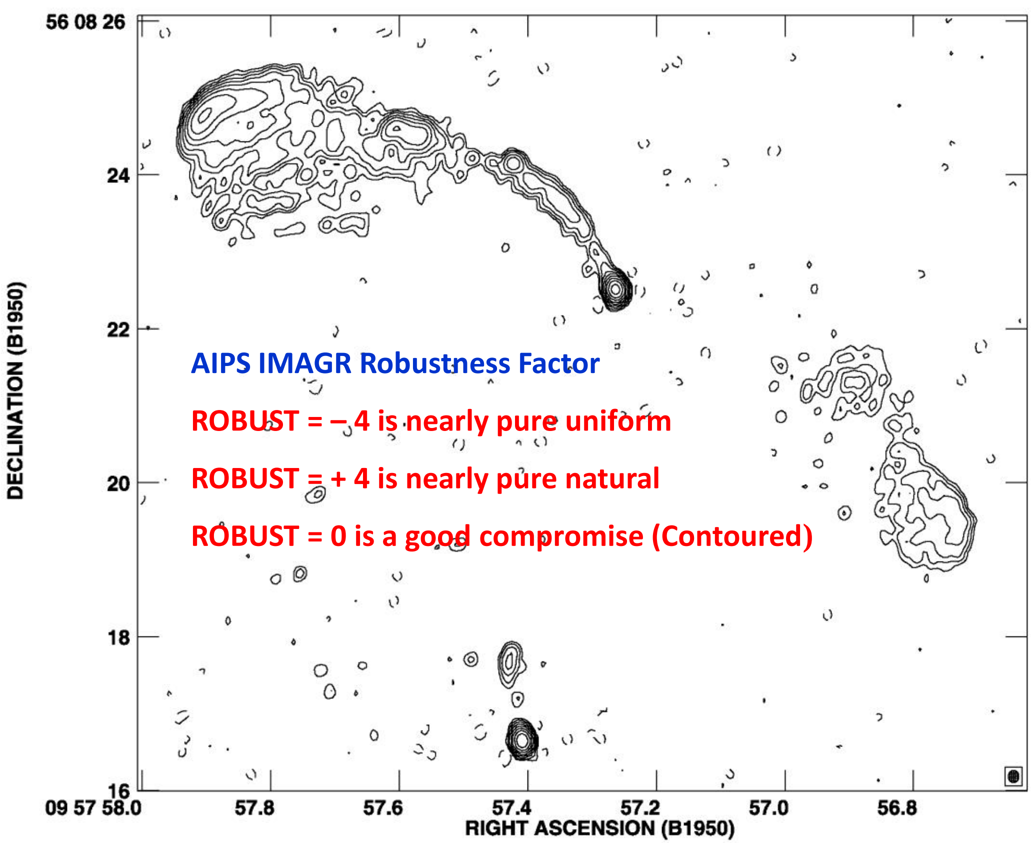

Modifies the variations in effective weight found in uniform weighting → more efficient use of data & lower thermal noise

Selecting a mid-range robustness factor can produce images close to uniform weighting resolution with noise levels close to naturally-weighted images

Imaging: Data Weighting by Telescope

Data from heterogeneous (mixed-type) arrays like the EVN, should be re-weighted by telescope sensitivity in order to minimise thermal noise


Arecebo 300m


Bonn 100m


Lovell 76m


SRT 64m


Westerbork 25m (93m)


Shanghai 65m


Yebes 40m

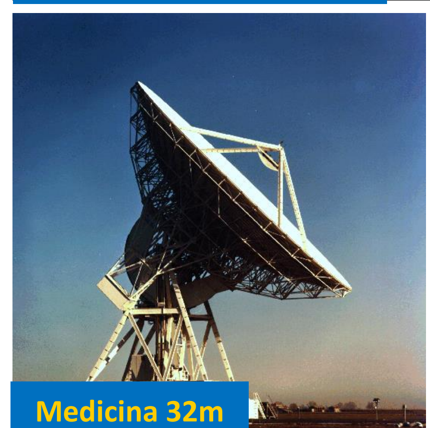
Medicina 32m

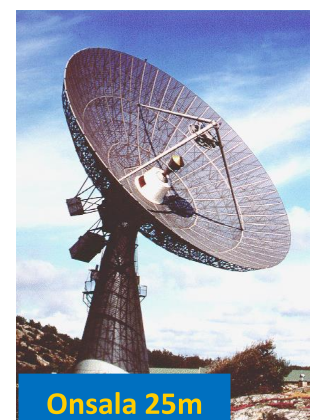
Onsala 25m

Imaging: Data Weighting by *u-v* Distance

RadioNet

Gaussian *u-v* taper or *u-v* range can smooth the image but at the expense of sensitivity since data are excluded or data usage is non-optimum

For arrays with sparse coverage beware compromising image quality by severely restricting the *u-v* coverage

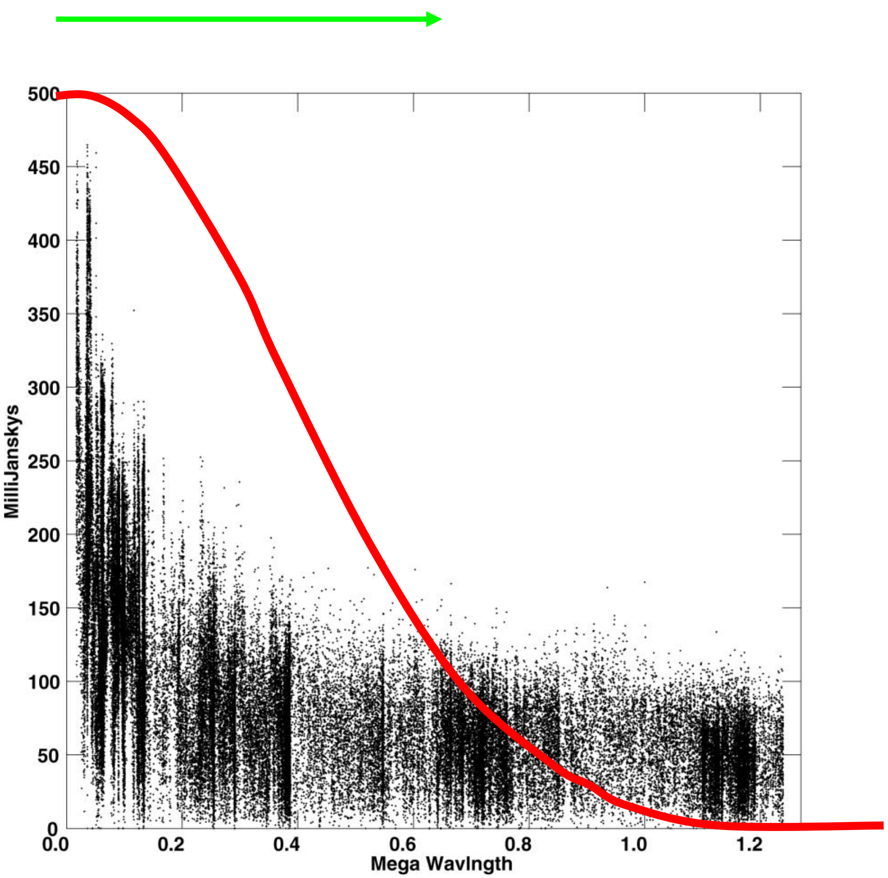

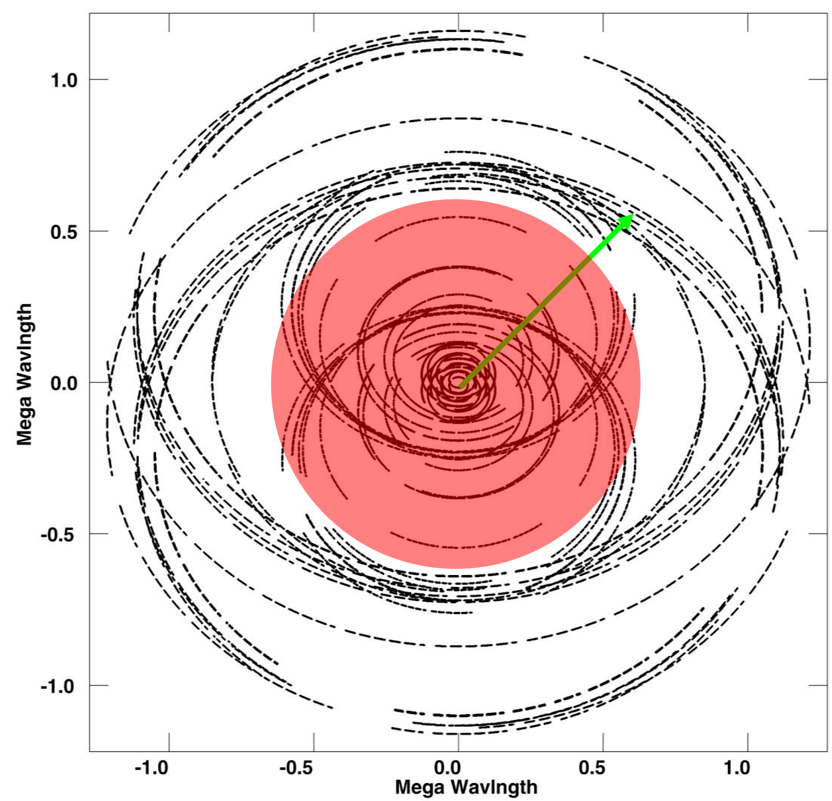

Wide-Field Imaging

Images with large numbers of resolution elements across them

Multiple images distributed across the interferometer primary beam

– M82 MERLIN MFS+VLA 5GHz image >1000 beams wide

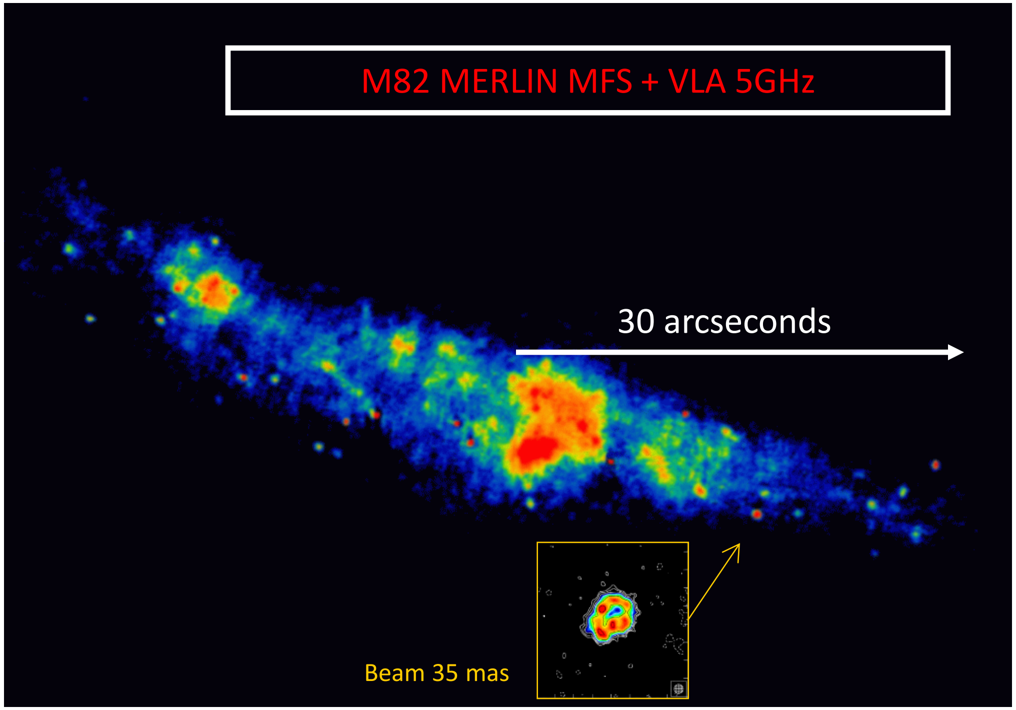

Wide-field images are subject to a number of possible distortions:

Non-coplanar baselines

Bandwidth smearing

Time-averaging smearing

Primary beam response

Wide-Field Imaging

Non-coplanar baselines

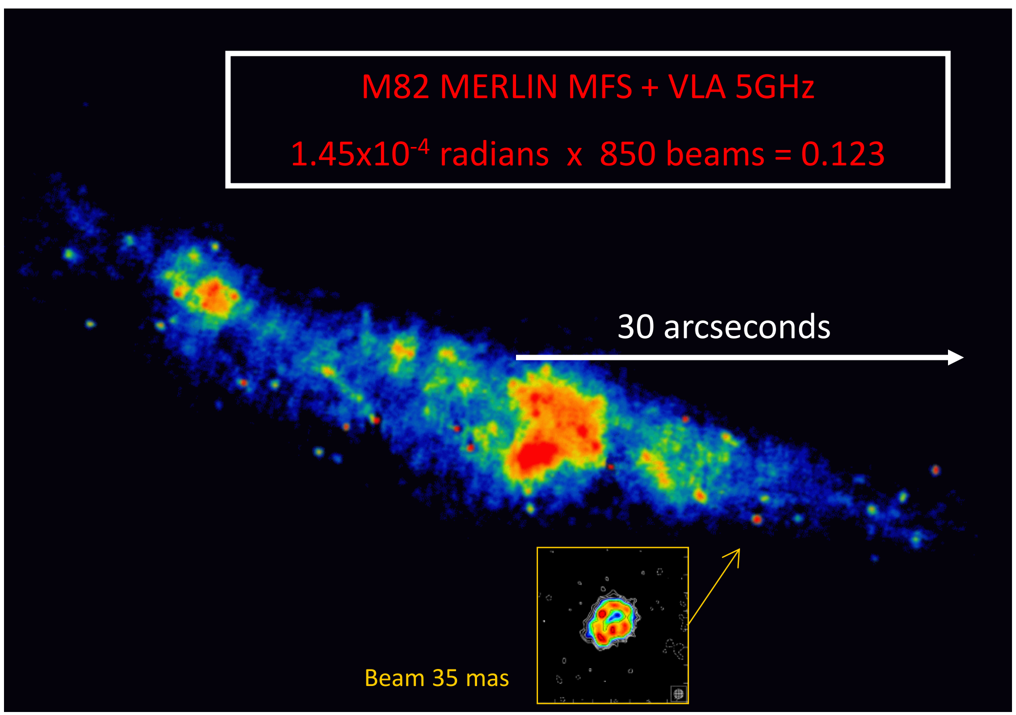

Standard Fourier synthesis assumes planar arrays – only true for E-W interferometers

Errors increase quadratically with offset from phase-centre

Serious errors result if

$\theta_{\text{offset}}(\text{radians}) \times \theta_{\text{offset}}(\text{beams}) > 1$

Need to account for a three-dimensional coherence function $V(u, v, w)$ *FT*→ $I(l, m, n)$ image vol.

– computationally expensive

Wide-Field Imaging

Non-coplanar baselines

Computationally simple method of imaging → a faceted or small field approximation in which the image sphere is approximated by pieces of many smaller tangent planes. The centre of each sub-field is correctly positioned in the three-dimensional image plane.

Within each sub-field fast two-dimensional FFTs may be used.

Errors increase quadratically away from the centre of each sub-field, but these are acceptable if enough small sub-fields are selected.

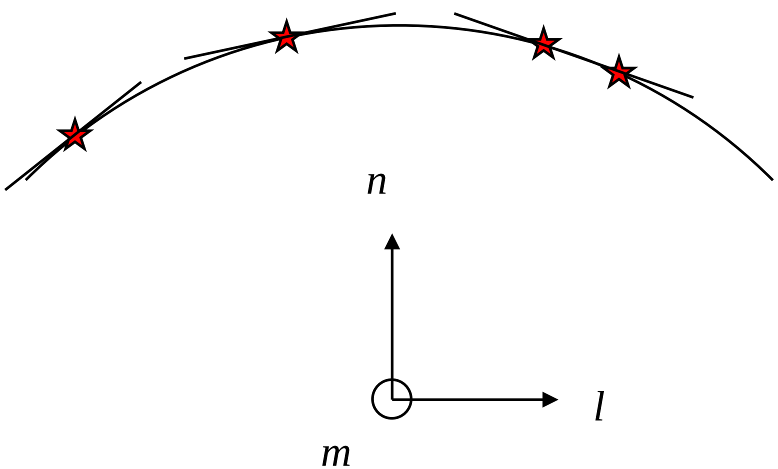

Facets can be selected so as to cover known sources.

Facets may overlap allowing complete coverage of the primary beam.

Wide-Field Imaging W-Projection

Facetted imaging naturally allows spatially dependent correction – separate telescope solutions for each facet

An alternative to multiple facets has been developed: W-projection

W-projection allows the projection of each *uvw* visibility onto a single 2-D *uv*-plane (*w*=0) with a phase shift proportional to the distance from the flat plane

Each visibility is mapped to all the *uv* points lying within a cone whose full angle is equal to the field of view of the required wide-field image – now with position-dependent errors

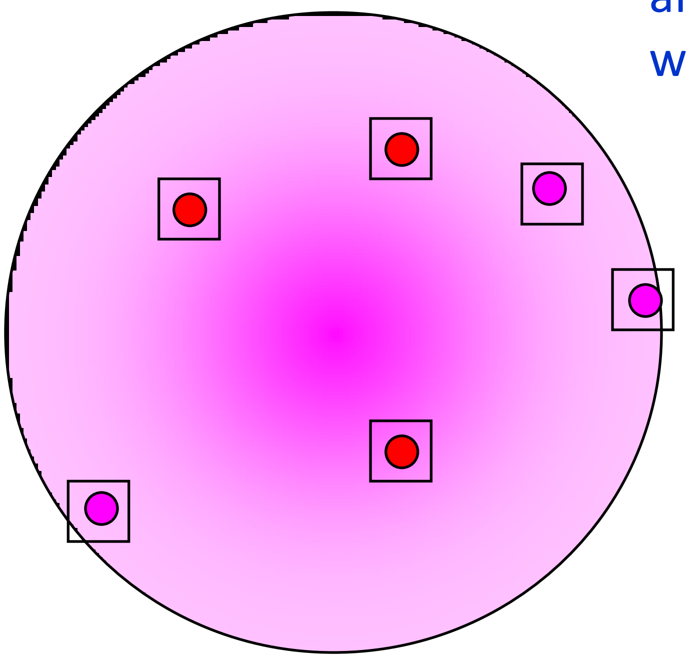

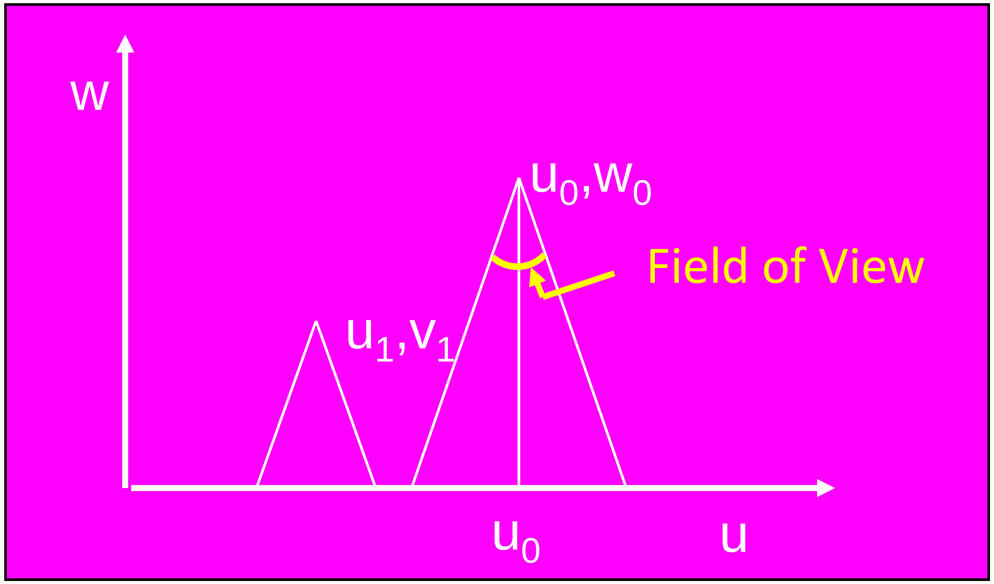

Wide-Field Imaging

Bandwidth smearing (chromatic aberration)

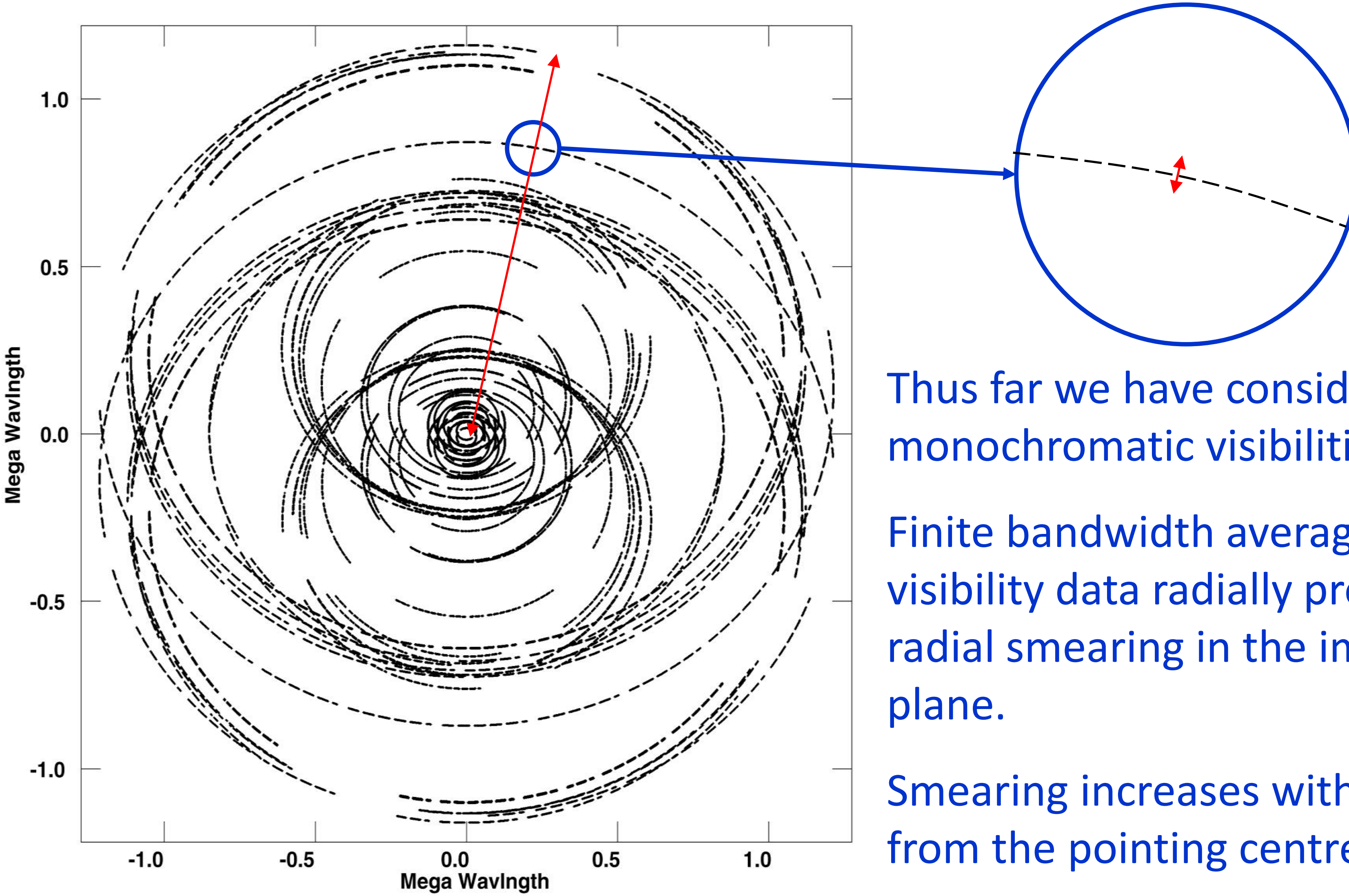

Thus far we have considered monochromatic visibilities.

Finite bandwidth averages the visibility data radially producing a radial smearing in the image plane.

Smearing increases with distance from the pointing centre.

Wide-Field Imaging

Bandwidth smearing

Bandwidth smearing (chromatic aberration) will produce radial smearing and reduction in source peak

Parameterized by the product of the fractional bandwidth (per channel) and the source offset in synthesised beam widths

$$\boxed{\delta\upsilon / \upsilon_0 \;\; x \;\; \theta/\theta_{HPBW}}$$

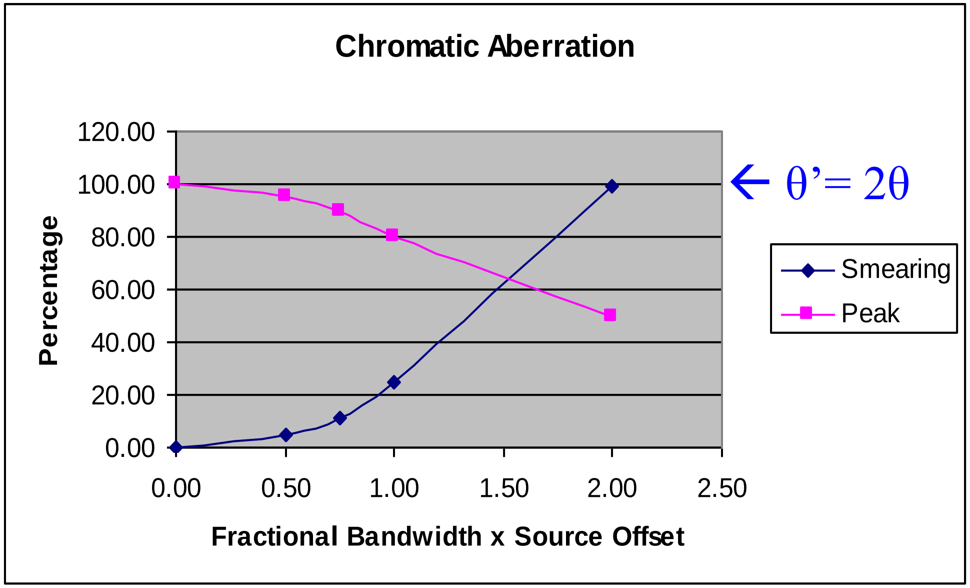

Can be alleviated by observing and imaging in spectral line mode with many narrow frequency channels gridded separately prior to Fourier inversion – reduces $\delta\upsilon$

– now practicable with new powerful correlators without the limitations of previous generations of correlator

Wide-Field Imaging

Bandwidth smearing

Historical VLA bandwidth smearing – 1.4GHz data with 50MHz bandwidth

Even with new EVLA data, take care with wide-field combination imaging – on edge of primary beam image may be ok at EVLA resolution but radially smeared at higher angular resolution....

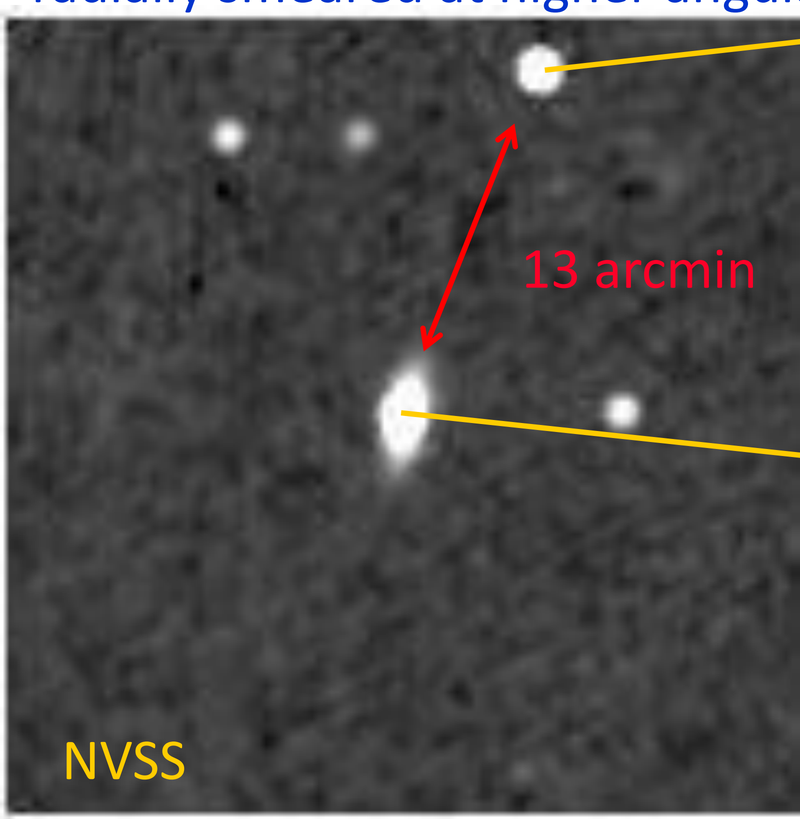

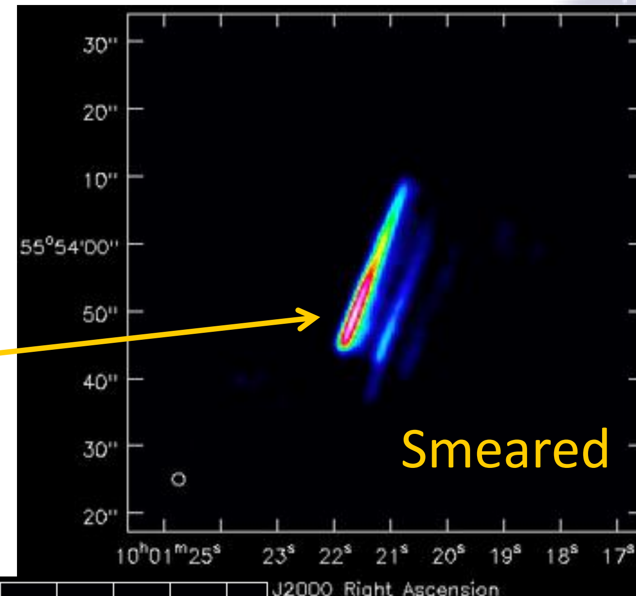

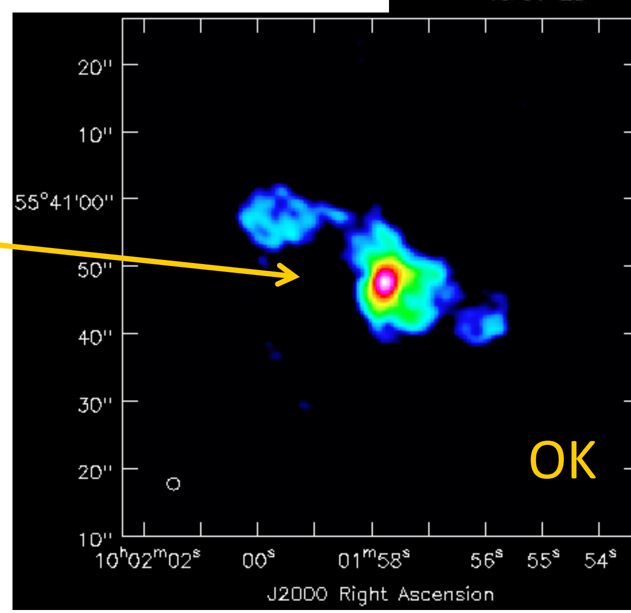

Wide-Field Imaging

Time-averaging smearing

Time-average smearing cannot be easily parameterized

Can be alleviated by ensuring that δt_{int} is small enough such that there at least 4 samples per turn of phase:

→Source offset from pointing centre ~10,000 resolution elements

→Assume 10,000 turns of phase on longest baselines in 6 hours

→Require 40,000 samples in 6 hours → δt_{int} ~0.5secs

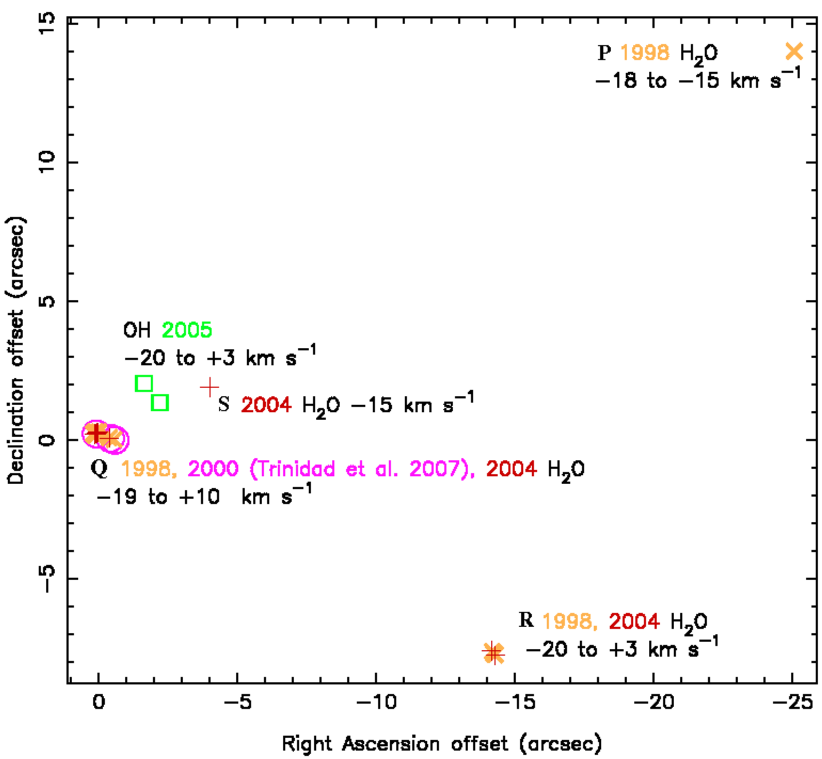

MERLIN 22GHz H_2O maser emission – 4 sec integration

Q – Pointing centre

R – ~2000 beams offset

Q – ~4000 beams offset

Can produce spurious multiple components….

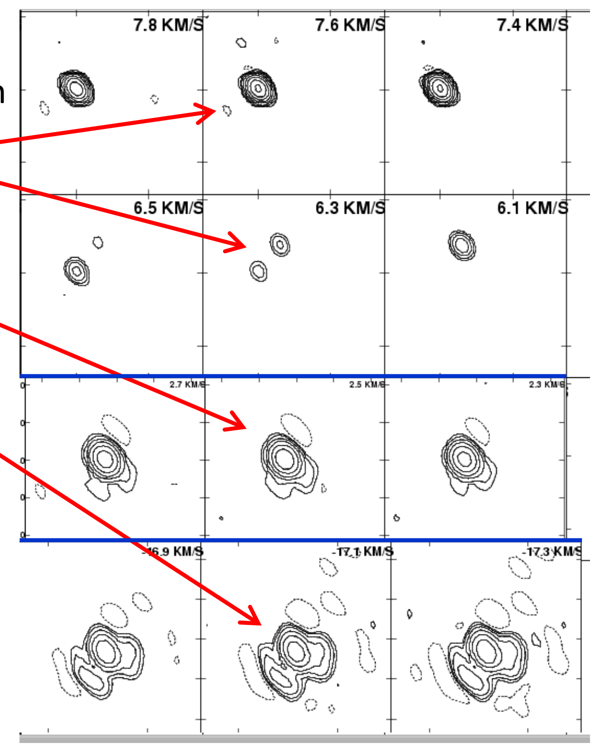

Wide-Field Imaging

Primary beam response

The ultimate factor limiting the field of view is the diffraction limit of the individual antennas.

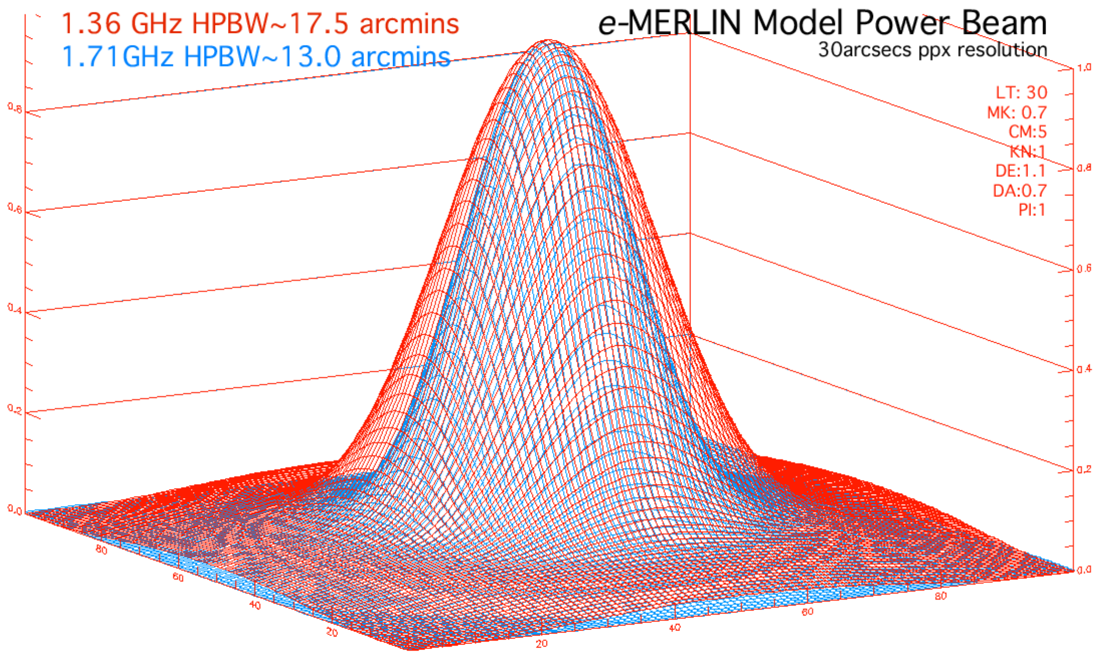

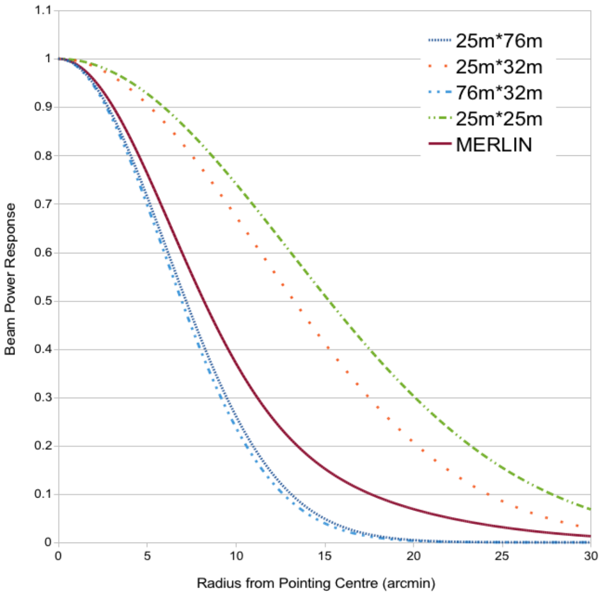

The overall correction will depend on the relative weighting and the data distribution between telescopes – & the types and sizes of the telescopes.

Primary beam will be frequency dependent.

Wide-Field Imaging

Confusion

Radio sources on the edge of the primary beam give rise to ripples in the centre of the field of view – subtract them out

The primary beam size is spectrally dependent, so image subtraction should include such corrections and be performed in full spectral-line mode

Pointing errors will introduce gain and phase changes on the edge of the primary beam. If severe, the apparent source structure may change – attempt multiple snapshot subtraction on timescales comparable with pointing error changes

OK for weak confusing sources

For stronger confusing sources……

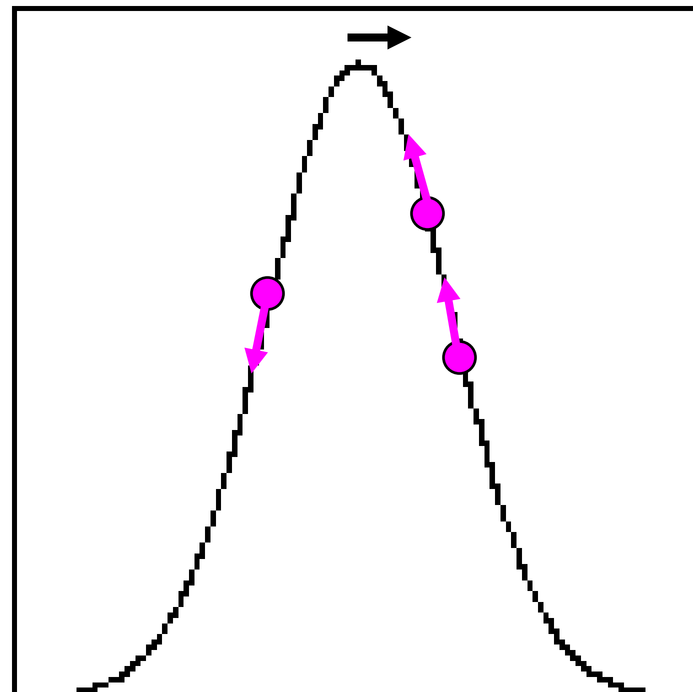

Wide-Field Imaging

Peeling away confusion

After phase calibrating the data, perform self-calibration for the brightest confusing source – then subtract it out

Delete phase solutions derived for previous confusing source ❶

Move to next brightest confusing source, perform self-calibration/imaging cycles – then subtract that source from the dataset ❷

Perform ❶and ❷ until all confusing sources are subtracted. Delete all self-calibration solutions and image central regions

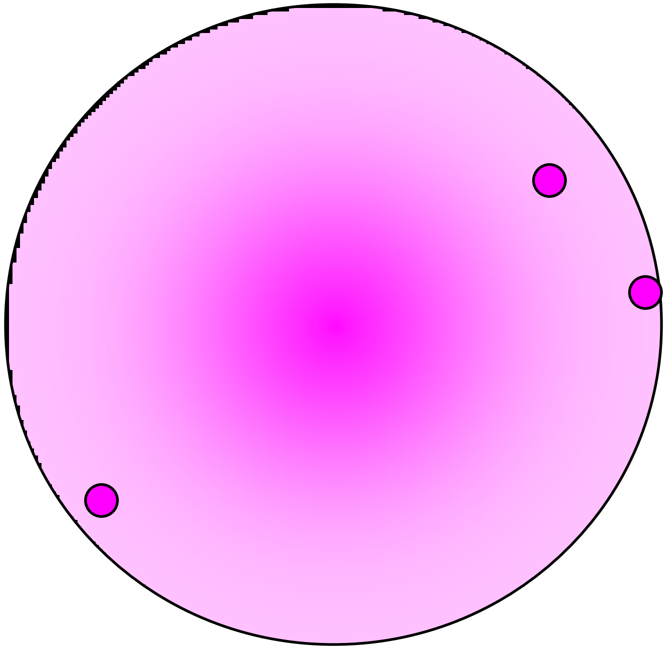

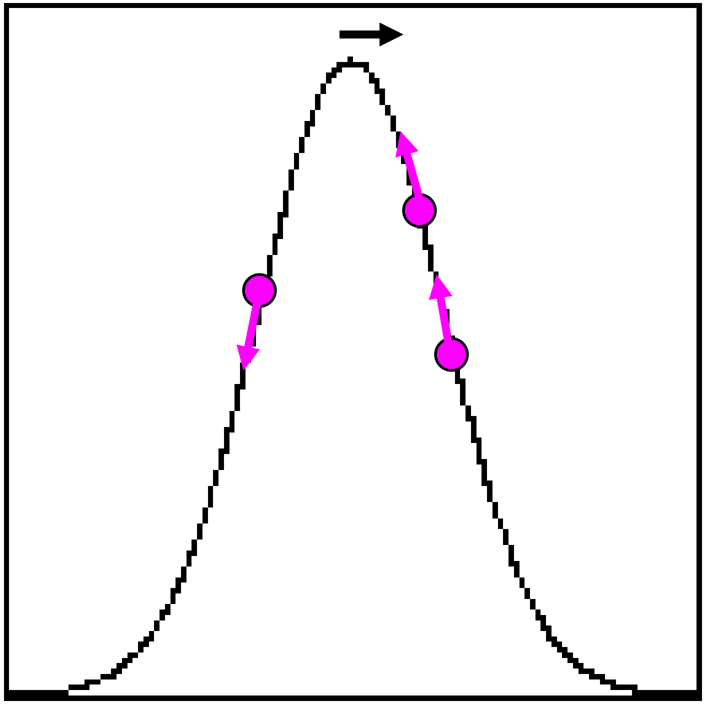

Wide-Field Imaging

In-beam self-calibration

After peeling off confusing sources, other sources may lie within the central areas of the primary beam

- Provided these are compact and bright enough, they can be used to self-calibrate the target (if they lie within the isoplanatic region of the image).

- For non-isoplanatic situations (eg VLA D-array at low frequencies, LOFAR) new routines are under development to solve for direction dependent telescope errors – provided there are enough sources to adequately sample the beam

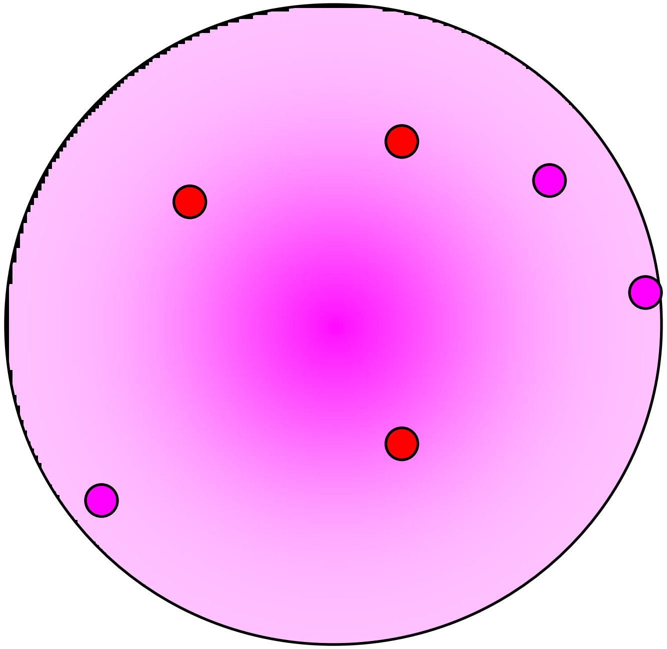

– LOFAR phase corrections derived for a number of in-beam phase reference sources

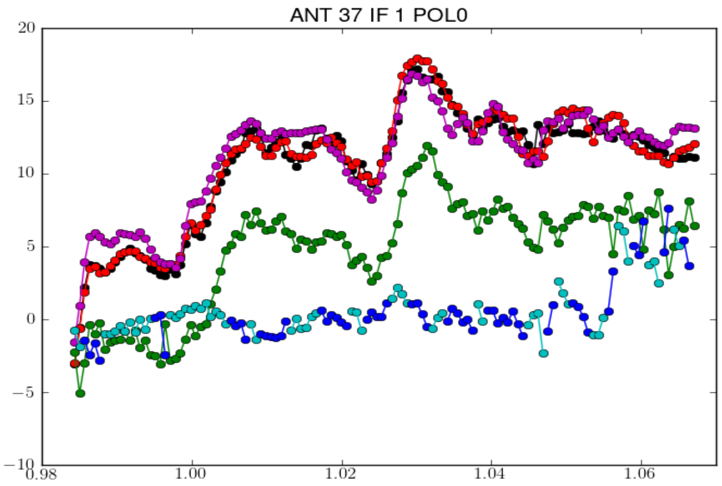

Multi-Frequency Synthesis

New wide-band telescopes (*e*-MERLIN, JVLA)large fractional bandwidths will require a spectral solution in addition to the radio brightness at each location in the image – Multi-Frequency Synthesis (MFS)

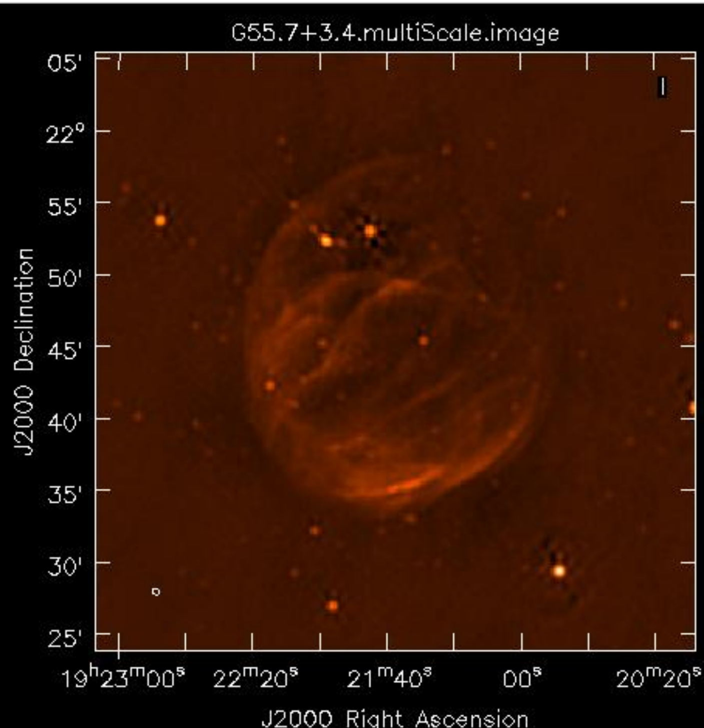

Multi-scale clean

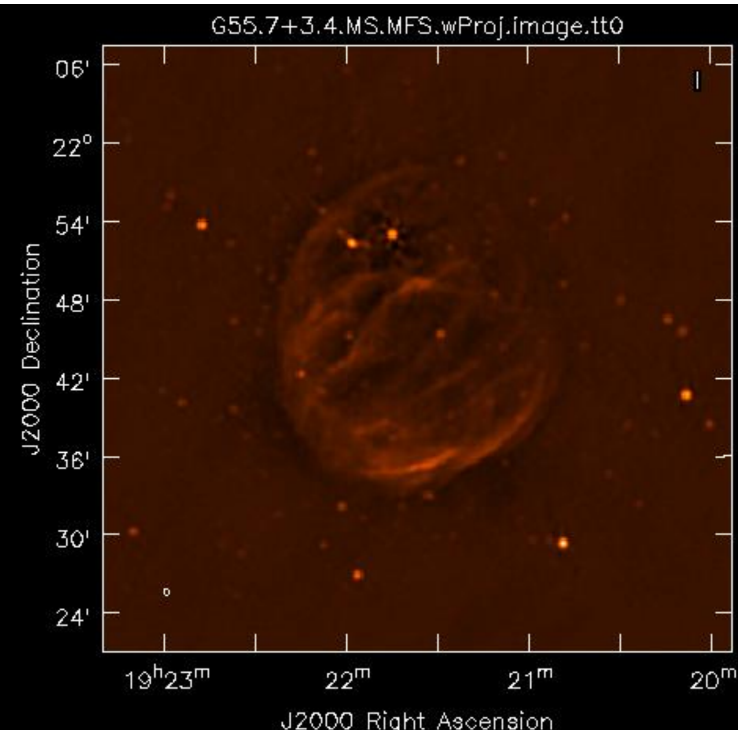

W-Projection, Multi-scale clean, MFS

Multi-Frequency Synthesis

New wide-band telescopes (*e*-MERLIN, JVLA)large fractional bandwidths will require a spectral solution in addition to the radio brightness at each location in the image – Multi-Frequency Synthesis (MFS)

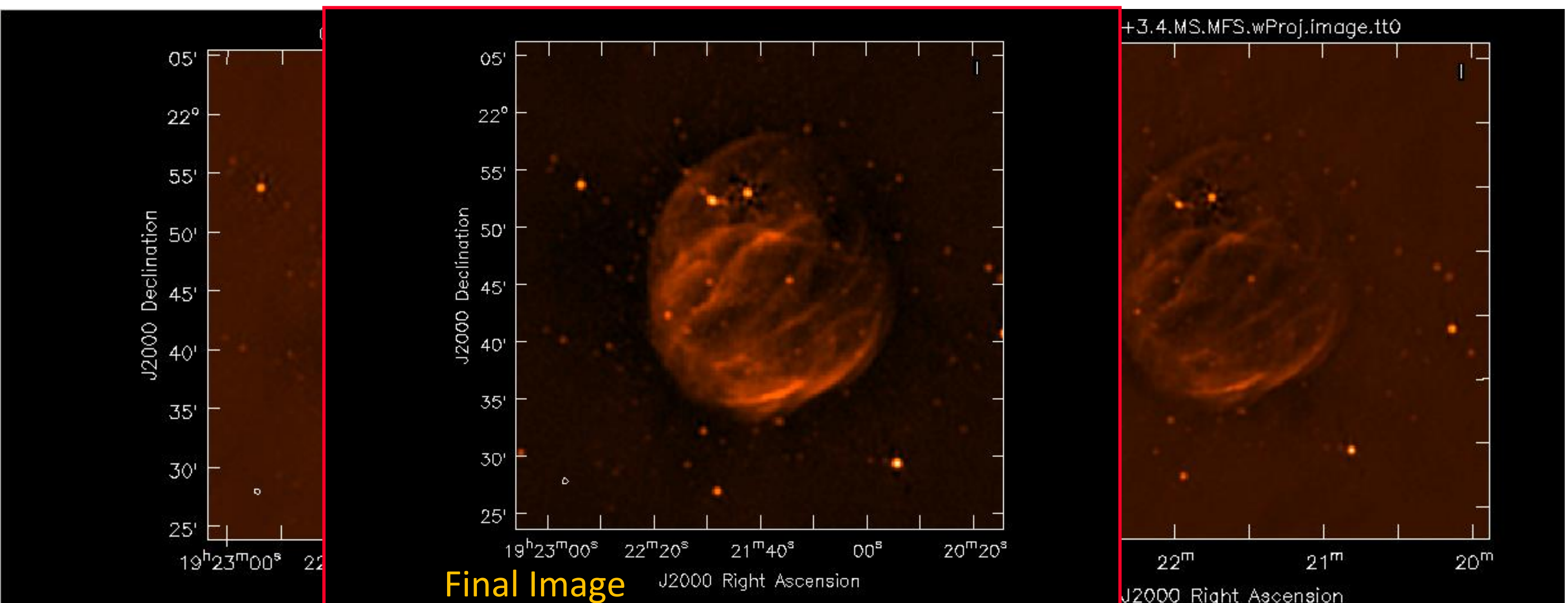

Multi-scale clean

W-Projection, Multi-scale clean, MFS

Multi-Frequency Synthesis

For JLVA & *e*-MERLIN MFS at C-& L-Band, fractional bandwidth is substantial: eg 4 – 8 GHz at C-Band.

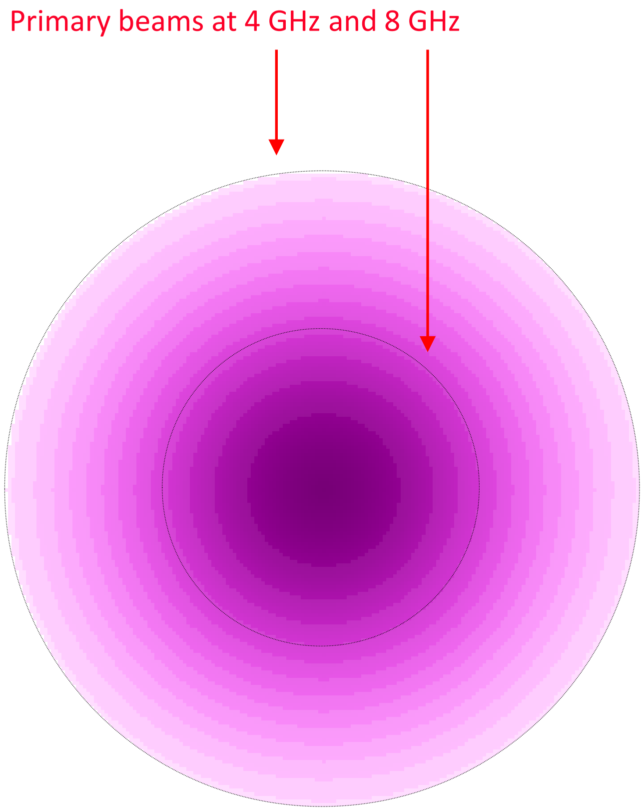

The size of the primary beam scales as 1/observing frequency

Full MFS imaging is restricted to the primary beam at the highest frequency

High dynamic-range confusion subtraction from outer parts of the primary beam is likely to be a challenging problem – will need ‘peeling’ in spectral-line mode, possibly in multi-snapshot mode.

Mosaicing

For single pixel receivers ultra-wide fields of view can be built up by mosaicing with multiple pointing centres

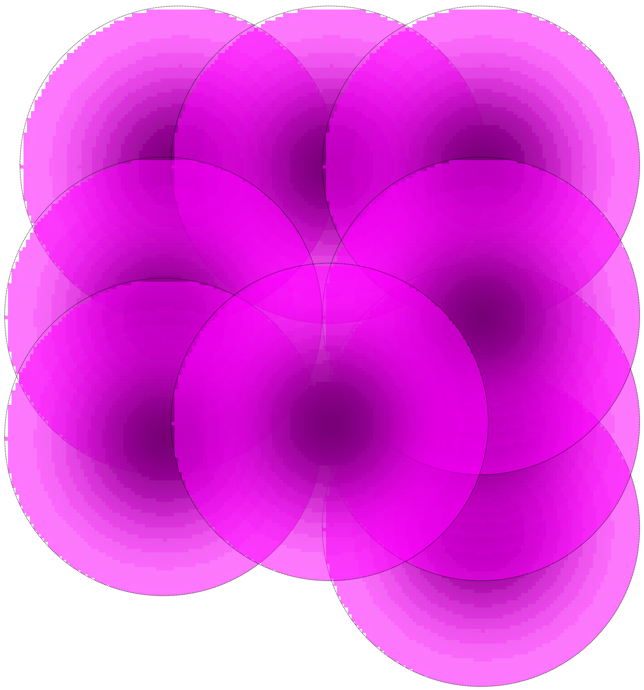

Each pointing centre must contain some degree of overlap.

Overlap optimisation depends on desired consistency in sensitivity across the mosaiced image and speed of observation.

For arrays with a single type of element, this is relatively straightforward – a typical compromise is a hexagonal pattern with a beam throw of ~60 %

For heterogeneous arrays, beam throw set by largest diameter antenna

Extended Fields of View: Aperture plane arrays

Replacing single pixel receivers with aperture plane arrays can dramatically increase area covered (x25) in a single observation – Aperture Tile In Focus (Apertif) is now being installed on the Westerbork array

→ Major increase in survey speed

Large numbers of overlapping beams – each separately correlated → large area coverage but with associated large datasets

ASKAP Phased Array Feed (PAF) area 1.4GHz coverage 1→30 square degrees

Extended Emission: Missing short-spacing data

Interferometer images with missing short-spacing data are to images set in a 'negative bowl' ($S_{uv=0}$ ~0)

Important for images of bright regions within large extended emission

Very short-spacing or single dish data added in either the *uv*-plane or the image plane

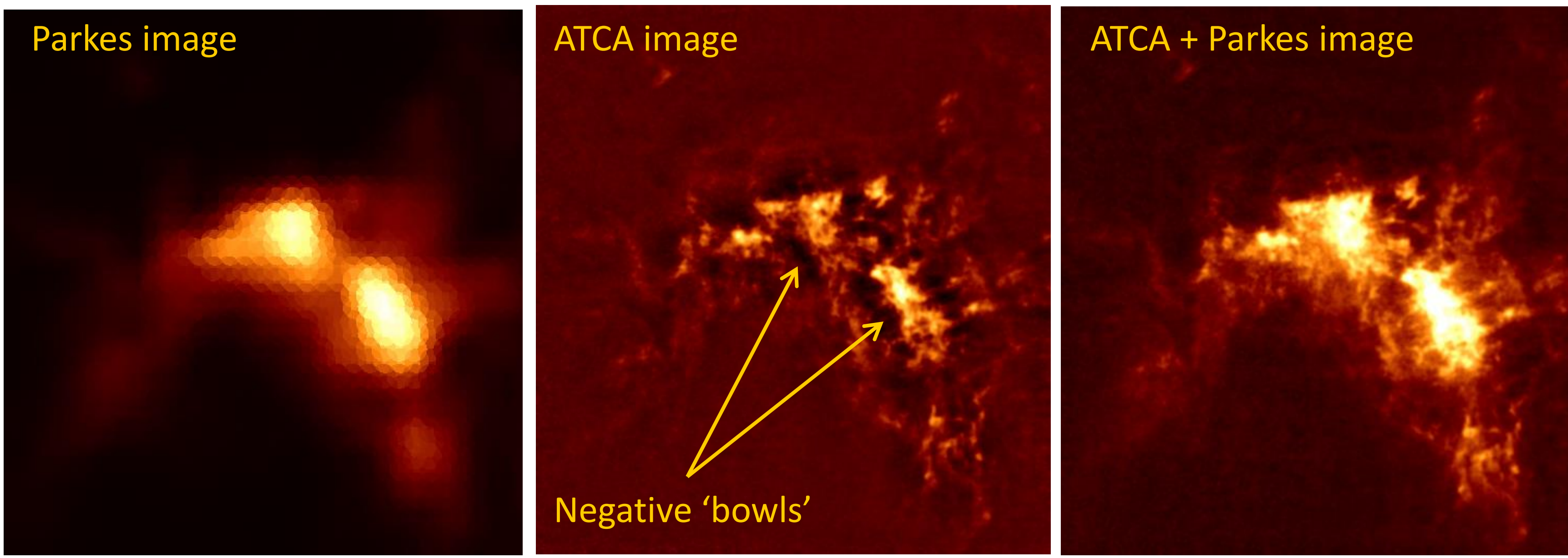

Image plane: Raw images combined + Beams combined → then deconvolved

HI in Small Magellanic Cloud
Single Dish: Parkes (D=64m)
Interferometer: ATCA (d=22m), Baseline min=34m

Stánimirovic et al, 1999

High Dynamic Range Imaging

Present dynamic range limits (on axis):

Phase calibration – up to 1000 → improve with self-calibration

Non-closing data errors – continuum ~20,000 line >100,000

After non-closing error correction <10,000,000

Redundant baseline data can help.....

Non-closing errors thought to be dominated by small changes in telescope passbands

Spectral line data configurations are the default for all new wide-band radio telescopes

In order to subtract out confusion we will need to be able to image with these very high dynamic ranges away from the beam centre

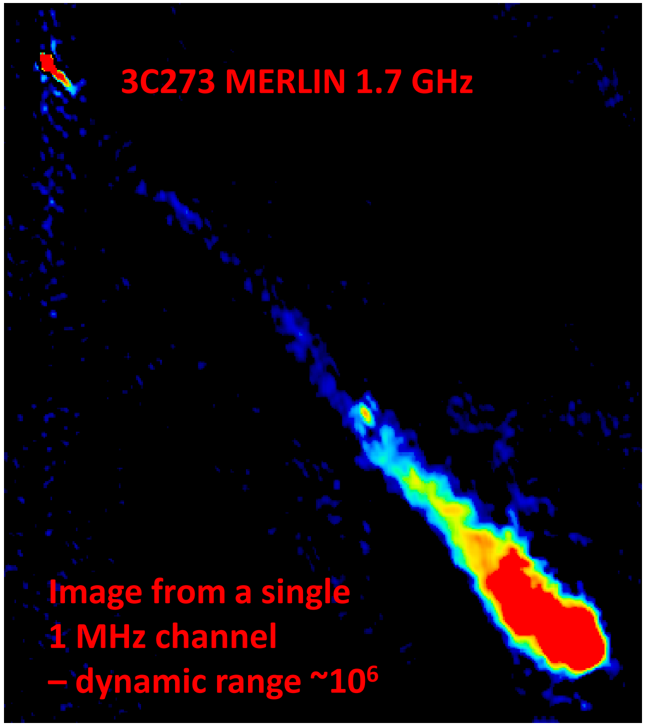

High Dynamic Range Imaging

Achieving high dynamic range off axis:

Monitor and calibrate your spectral line data for dynamically changing spectral band-pass effects.

Correct for primary beam response to very high precision well into the near side-lobes

Tests with ATCA data have successfully achieved high dynamic ranges off axis with accurate beam models out to 3rd sidelobe of the primary beam….

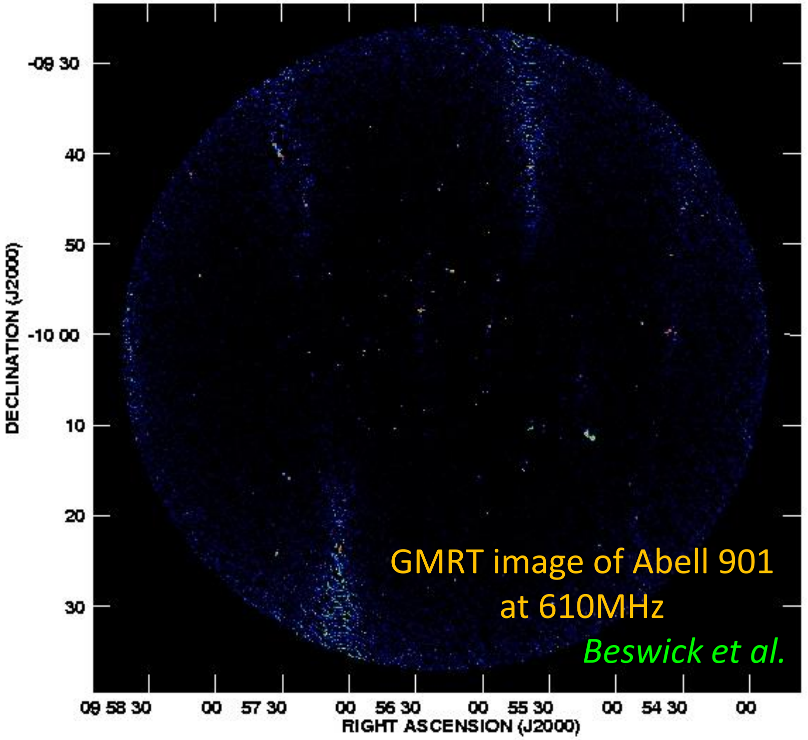

Off axis imaging will continue to be challenging – but very high fidelity wide-field imaging close the beam centre is now routine

High Dynamic Range Imaging

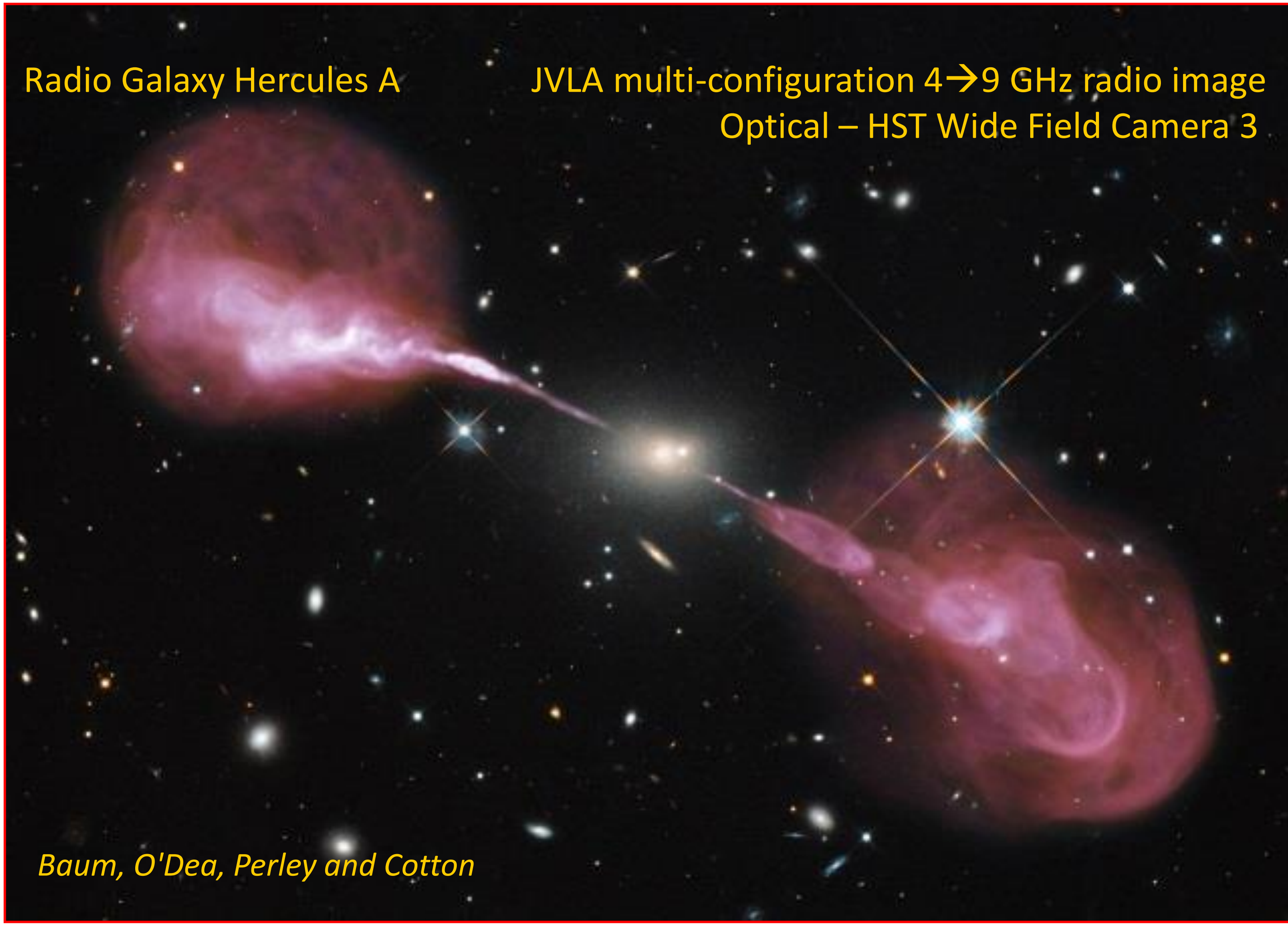

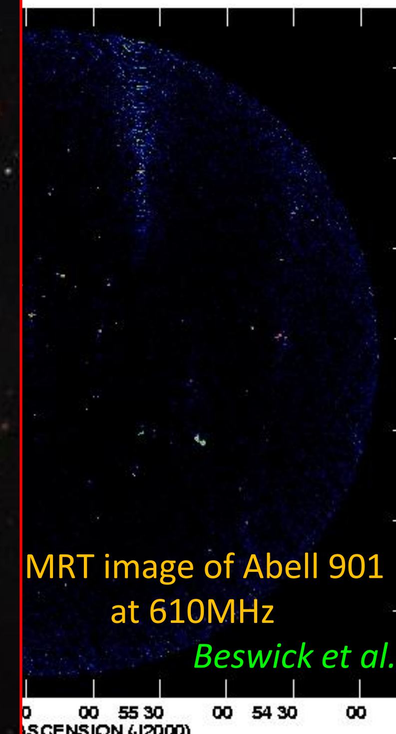

Off axis imaging will continue to be challenging – but very high fidelity wide-field imaging close the beam centre is now routine